Augusto Finger Pacheco

ANALYSIS AND REDUCTION OF DETAILED CHEMICAL KINETICS MECHANISMS FOR COMBUSTION OF ETHANOL AND AIR

Dissertação submetida ao Programa de Pós-Graduação em Engenharia Mecânica da Universidade Federal de Santa Catarina para a obtenção do Grau de Mestre em Engenharia Mecânica
Orientador: Prof. Amir Antônio Martins de Oliveira Jr. Ph.D.

Florianópolis
2016

Ficha de identificação da obra elaborada pelo autor,
através do Programa de Geração Automática da Biblioteca Universitária da UFSC.

Pacheco, Augusto Finger
ANALYSIS AND REDUCTION OF DETAILED CHEMICAL KINETICS MECHANISMS FOR COMBUSTION OF ETHANOL AND AIR / Augusto Finger Pacheco ; orientador, Amir Antônio Martins de Oliveira Jr. - Florianópolis, SC, 2016.
120 p.

Dissertação (mestrado) - Universidade Federal de Santa Catarina, Centro Tecnológico. Programa de Pós-Graduação em Engenharia Mecânica.

Inclui referências

1. Engenharia Mecânica. 2. Ethanol. 3. Combustion. 4. Chemical Kinetics. 5. Reduction Methods. I. de Oliveira Jr., Amir Antônio Martins . II. Universidade Federal de Santa Catarina. Programa de Pós-Graduação em Engenharia Mecânica. III. Título.

Augusto Finger Pacheco

ANALYSIS AND REDUCTION OF DETAILED CHEMICAL KINETICS MECHANISMS FOR COMBUSTION OF ETHANOL AND AIR

Esta Dissertação foi julgada adequada para obtenção do Título de "Mestre",e aprovada em sua forma final pelo Programa de Pós Graduação em Engenharia Mecânica.

Florianópolis, 19 de julho de 2016.

_____

Prof. Armando Albertazzi Golçalves Jr., Dr. Eng.
Coordenador do Curso

_____

Prof. Amir Antônio Martins de Oliveira Jr., Ph.D.
Orientador
Universidade Federal de Santa Catarina

Banca Examinadora:

_____

Prof. Luis Fernando Figueira da Silva, Dr.Eng.
Pontifícia Universidade Católica do Rio de Janeiro

_____

Profa. Cintia Soares, Dr. Eng.
Universidade Federal de Santa Catarina

_____

Prof. Leonel Rincon Cancino, Dr.Eng.
Universidade Federal de Santa Catarina

RESUMO EXPANDIDO

Introdução

Com o aumento nos desafios para o desenvolvimento de estratégias sustentáveis para controle de emissões, principalmente no setor automotivo, muitos recursos têm sido empregados para aumentar a eficiência dos sistemas veiculares, como estratégias *Start-Stop*, e abordagens avançadas no controle da combustão, como a combustão no modo HCCI - *Homogeneous Charge Compression Ignition*.

A combustão em HCCI é caracterizada pelo controle de ignição e taxa de liberação de energia pela cinética química do combustível empregado. Para o projeto e otimização desses sistemas, as ferramentas computacionais com o emprego de modelos de cinética química detalhada apresentam-se com excelente custo-benefício quando comparadas com desenvolvimentos puramente experimentais. Entretanto, o custo computacional do emprego de grandes mecanismos cinéticos tende a inviabilizar a sua utilização na simulação de geometrias e condições de operação reais de motores. Assim, a utilização de mecanismos menores, ditos reduzidos, os quais ainda reproduzem as características desejadas da combustão dentro de margens de erro aceitáveis tornam-se indispensáveis.

Objetivos

Aplicar métodos de redução de mecanismos cinéticos detalhados; desenvolver um algoritmo para a redução automatizada; analisar a taxa de redução e o desempenho relativo desses diferentes métodos; obter mecanismos reduzidos usando como alvos da redução a velocidade de chama laminar e o atraso de ignição, sujeito à determinados limites de erro; e analisar a estrutura final do mecanismo e caminhos de reação principais visando a otimização dos mecanismos cinéticos existentes.

Materiais e Métodos

Este trabalho enfoca os mecanismos cinéticos detalhados para a combustão de etanol. Dentre os mecanismos existentes, foram selecionados três, desenvolvidos originalmente visando alvos diferentes. O primeiro, desenvolvido por Leplat, 2011, apresenta 38 espécies e 252

reações, incluindo ainda dados de propriedades de transporte, e foi principalmente desenvolvido utilizando medições em reator perfeitamente misturado. O Segundo, desenvolvido por Cancino, 2010, possui 135 espécies e 1349 reações. Além do mecanismo de oxidação do etanol há ainda a inclusão do mecanismo de oxidação do nitrogênio. Foi desenvolvido visando a reprodução de atraso de ignição em tubo de choque. Já o último mecanismo selecionado foi o apresentado por Mittal, possuindo 111 espécies e 710 reações. Como o mecanismo do Leplat, este possui dados de propriedades de transporte e não apresenta mecanismo do nitrogênio. Foi desenvolvido originalmente buscando a reprodução de atraso de ignição medido em máquina de compressão rápida.

As estratégias para a redução englobam muitas análises diferentes a respeito de como os resultados se comportam frente as reações (como a análise de sensibilidade, DSA, ou o índice de taxa de produção, ROP) ou ainda como as espécies estão ligadas entre si (gráfico de relação direta, DRG, e suas variações como o DRGEP e o PFA).

Resultados

O primeiro mecanismo a ser submetido a redução foi o mecanismo proposto por Leplat. Por apresentar um número de espécies e reações reduzido comparado aos outros, cinco mecanismos foram obtidos, utilizando os seguintes métodos de redução: DSA, ROP, DRG, DRGEP e PFA. O processo foi realizado utilizando dados de taxa de reação de um modelo de propagação de chama livre. Dos mecanismos obtidos, o DSA apresentou a maior redução no numero de reações enquanto o DRGEP produziu o mecanismo com o menor número de espécies.

Da resposta do mecanismo detalhado aos métodos empregados, apenas os métodos baseados em espécies, DRG e DRGEP, foram selecionados para serem aplicados nos mecanismos maiores. Tal decisão foi motivada pela presença de velocidades elevadas de redução e facilidade na sua aplicação.

Para o mecanismo do Cancino, três mecanismos reduzidos foram obtidos, usando duas abordagens diferentes do método DRG e um empregando o DRGEP. Além disso, apenas as espécies do mecanismo de oxidação do etanol foram avalidas e removidas, mantendo o mecanismo do nitrogênio completo. O mecanismo reduzido final

apresenta 79 especies e 821 reações contra as 135 especies e 1349 reações do mecanismo original. Para a redução, apenas dados de taxa de reação de um modelo de pressão contante foram utilizados.

Finalmente, o terceiro mecanismo, proposto por Mittal, foi reduzido, utilizando desta vez apenas o método DRG e o DRGEP. O mecanismo obtido via DRG apresentou a maior redução, com 41 especies e 240 reações contra as 111 especies e 710 reações do mecanismo original. O mecanismo obtido via DRGEP por sua vez apresentou 46 especies e 303 reações. O mesmo modelo utilizado para o mecanismo do Cancino foi utilizado para gerar os dados de taxas de reação para a redução do mecanismo detalhado proposto por Mittal.

Como passo final, uma avaliação dos mecanismo foi realizada. Na questão da sensibilidade, todos os mecanismos reduzidos finais mantiveram as mesmas reações como as mais importantes, manteendo assim o núcleo do mecanismo intacto. Já ao observar a evolução dos mecanismos reduzidos utilizando o método DRG em cada ponto, observamos que, no caso do mecanismo proposto por Leplat, é necessário um número maior de espécies no espaço delimitado pela espessura de chama. Já para o atraso de ignição, duas condições diferentessão observadas. A primeira, ao avaliar o mecanismo do Cancino, há um aumento do número de especies até próximo ao IDT, enquanto que, para o mecanismo do Mittal, há a necessidade de maiores mecanismos no inicio do processo de oxidação. Tal diferença pode ser atribuída ao fato de que o mecanismo apresentado por Mittal apresentar um número de espécies reativas muito maior do que as presentes do mecanismo do Cancino. Porém, próximo à ignição a situação é inversa, ou seja, o mecanismo proposto por Cancino apresenta uma maior necessidade de espécies do que proposto por Mittal. Tal condição pode estar associada ao método empregado para a contrução dos mecanismos e ainda à presença do sub-mecanismo para a oxidação do nitrogênio. Tais influências ainda necessitam de estudos adicionais.

Conclusão

À respeito dos mecanismos finais, houve uma redução no número de espécies, variando de 87% do número inicial de espécies (obtido através da aplicação do DRGEP no mecanismo proposto por Leplat) até 37% (obtido com o emprego do DRG no mecanismo proposto por Mittal). As reduções utilizaram um limite máximo de erro no parâmetro avaliado de até 5%, mantendo os resultdos obtidos com a

aplicação dos mecanismos reduzidos dentro de uma margem aceitável de erro.

No que tange os métodos empregados, aqueles com as maiores taxas de remoção de espécies foram aqueles basedos em espécies (principalmente o DRGEP e o DRG), atingindo taxas muito elevadas na remoção tanto de espécies como de reações. Ao avaliar os menores mecanismos obtidos, os métodos DRGEP e DRG, nesta ordem, apresentaram os menores mecanismos finais. Já para as reações, o DSA apresentou as maiores reduções.

Ao analisar o processo de oxidação através da utilização das sensibilidades das reações, todos os mecanismos reduzidos mantiveram as reações com os maiores valores de sensibilidade com seus coeficientes no mesmo patamar dos encontrados nos mecanismos detalhados, mantendo desse modo as pricipais reações nos mecanismos reduzidos.

Ainda na análise da combustão, mecanismos pontuais obtidos através do método DRG mostram a necessidade, em cada ponto da simulação, de um mecanismo cinético com números diferentes de espécies e consequentemente de reações. Partindo de tal análise, pode-se identificar zonas onde um mecanismo cinético ainda menor poderia representar o processo e zonas onde mais detalhe é necessário.

Assim, algumas propostas para trabalhos futuros são definidas. No que tange a redução de grandes mecanismos cinéticos, a utilização de métodos automatizados e que possam compreender diversos reatores simultaneamente (possuindo assim uma gama maior de condições de operação) é proposta. Ainda, a implementação de estratégias hibridas de redução, como por exemplo a utilização de DRGEP aliado à DSA pode ser utilizada para gerar mecanismos cinéticos ainda mais reduzidos.

A utilização de métodos de redução *on-the-fly* para a resolução de problemas de escoamentos reativos, principalmente em aplicações de CFD com turbulência se tornam interessantes.

ABSTRACT

In this work, three detailed kinetic mechanisms available in the literature were subjected to different methods of reduction, using the conditions found on internal combustion engines normal operation as reduction targets. The mechanisms selected were those of Leplat and co-workers (2011), from ICARE, Orleans, France, containing 252 reversible chemical reactions among 38 chemical species, developed mainly to reproduce measurements of species concentration in perfectly-stirred reactors; of Mittal and co-workers (2014), from C3-NUI, Ireland, involving 710 reversible chemical reactions among 111 chemical species, developed mainly to predict ignition delay time measured in rapid compression machine; and that of Cancino and co-workers (2010), from IVG, Germany, and UFSC, Brazil, involving 1349 reversible chemical reactions among 135 chemical species, mainly developed to predict high-pressure ignition delay time measured in shock tubes. The reduction methods selected were the Sensitivity Analysis (SA), Rate of Production (ROP), Directed Relation Graph (DRG) and Directed Relation Graph with Error Propagation (DRGEP) and Path Flux Analysis (PFA). Since Leplat's mechanism is the most compact, it was selected for the assessment of the final reduction and convergence ratio involved in each reduction method studied. Both ignition delay time and laminar flame speed, evaluated over a large range of temperature, pressure and equivalence ratios, were selected as reduction targets. The maximum difference allowed between the predictions of the full detailed and the reduced mechanisms was 5 % over the entire target range. From the initial analysis, the DRG and DRGEP methods appeared as the most effective, both in terms of the size of the final reduced mechanism, as well as in terms of the rate of removal of species. The DRG and DRGEP methods were then systematically applied to the other mechanisms and the differences observed in the reduced species were noted and analyzed. The final reduced mechanism obtained via DRGEP from Leplat´s mechanism presented, respectively, 84 % and 72 % of the species and reactions of the detailed mechanism. For the Cancino mechanism, the DRGEP produced a larger reduction with 58 % and 61 % of species and reactions respectively of the detailed mechanism, without removing the nitrogen oxidation mechanism and still representing the high-pressure IDT with a 5% difference from the detailed mechanism. Finally, for the Mittal mechanism, the DRG method presented the largest reduction, reaching 37% of species and 34% of reactions of the detailed mechanism. The sensitivity analysis of

the reduced mechanisms revealed the same group of most sensitive reactions in respect to the laminar flame and ignition delay time as the detailed mechanism, indicating that the reduction does not change the relative importance of the reactions within a reaction path for a given mechanism. However, when the reduced mechanisms are compared among them, several basic differences arise, mainly in the level of detail, expressed as the number of intermediates and reactions, placed in modeling early or late kinetics phenomena. These observations may lead to the development of more comprehensive mechanisms for the modeling of ethanol combustion.

Keywords: Combustion. Chemical kinetics. Ethanol. Biofuels.

LIST OF TABLES

LIST OF FIGURES

LIST OF ABBREVIATIONS AND ACRONYMS

CSP	Computational Singular Perturbation
CSTR	Continuous Stirred-Tank Reactor
CVR	Constant Volume Reactor
DRG	Directed Relation Graph
DRGEP	Directed Relation Graph with Error Propagation
DRGEPSA	Directed Relation Graph with Error Propagation and Sensitivity Analysis
DSA	Direct Sensitivity Analysis
EC-DAC	Error Controlled Dynamic Adaptive Chemistry
FPT	Flux Projection Tree
GA	Genetic Algorithm
IDT	Ignition Delay Time
ILDM	Intrinsic Low-Dimensional Manifold
JSR	Jet Stirred Reactor
LFB	Laminar Flat Burner
LFS	Laminar Flame Speed
NDSA	Normalized Direct Sensitivity Analysis
PCA	Principal Component Analysis
PE	Partial Equilibrium
PFA	Path Flux Analysis
PFR	Permanent Flow Reactor
PSR	Perfect Stirred Reactor
QSS	Quasi-Steady State
QSSA	Quasi-Steady State Analysis
RCM	Rapid Compression Machine

RFA	Reactivity Flux Analysis
ROP	Rate of Production
SA	Sensitivity Analysis
ST	Shock Tube

LIST OF SYMBOLS

ρ	Density
u_i	Velocity
p	Pressure
Y_k	Mass Fraction of Chemical Species
μ	Dynamic Viscosity
h	Enthalpy
D_k	Fick Diffusion Coefficient
$V_{k,i}$	Diffusion Velocity
λ	Thermal Conductivity
T	Temperature
$\dot{Q}$	Volumetric Energy Generation
$\dot{\omega}_k$	Reaction Rate
t	Time
k_f, k_r	Forward and Reverse Rate Constants
A	Pre-exponential Factor
E_A	Activation Energy
R_u	Universal Gas Constant
ν', ν''	Stoichiometric Coefficients
I_{AB}	Relation Importance Index
I_B	Specie Importance Index

SUMMARY

1. INTRODUCTION

1.1. Motivation

Combustion remains as the main form to produce energy in the world. According to EIA (2014) and BP (2014), 87 % of the primary energy in the world is produced by means of combustion. In 2012 the energy portion occupied by fossil fuels was of 82%, with a 2040 projection of 80%. The portion of renewable liquid fuels presents the higher growing rate and is projected to reach 12 % of the overall world energy consumption by 2040. The reduction on the liquid fossil fuel consumption is connected mainly to the increase in vehicle energy efficiency and the penetration of renewal fuels in the transport segment.

Brazil presents a much more renewable energy matrix than the remaining of the world (EPE, 2015). In 2012, 46 % of the primary energy was produced from renewable sources, in which wood and sugar cane accounts for 27 %. Adding all the consumption of oil (42 %), natural gas (9.3 %) and coal (0.8 %), we conclude that 80 % of the total energy in Brazil is converted by combustion processes. This includes most of the energy consumed in the industrial sector and all transportation fuels. The industrial and transportation sector account, respectively, for 39 % and 32 % of the total energy consumed in Brazil. To displace oil by biofuels in the transportation sector is a huge task, not reachable in the short term.

In order to limit the impact of pollution from the transportation sector, several legislation were passed in different countries, such as the Clean Air Act in US, the European Emission Standards on Europe and the PROCONVE in Brazil. In the vehicular segment, two paths for vehicle development became evident; the use of cleaner fuels, such as ethanol, and the search for more efficient technologies, both for vehicles and engines. When choosing a renewable fuel, several factors become relevant and of all, the economic and geographic limitations are the most important. In Brazil, the climate and the sugarcane culture influenced the use of ethanol as a substitute of gasoline. Besides, the use of ethanol as an anti-knock additive for gasoline is an important drive for the ethanol use in the world (Jeuland et al., 2004).

On the technology side, several approaches to control the emission levels for the automotive industry were developed. The start-stop and hybrid vehicles are examples of automotive system improvements. More advanced combustion control strategies, as the low

temperature combustion (LTC), which encloses the HCCI and its variations, are highlighted. As an example, Kokjohn et al. (2011) studied the concept of employing a dual fuel RCCI (Reactivity Controlled Compression Ignition), achieving a gross efficiency of 56 % and great reduction on NOx and soot level. The main control for this approach is highly based on the auto ignition property of the fuel used.

According to Kalghatgi (2014), the combustion, performance, efficiency and emissions of internal combustion engines are deeply connected to the autoignition property of the fuel. Experiments of ignition delay times in shock tubes and detailed models are being used to better understand the auto ignition process.

Autoignition is a property highly dependent of the chemical kinetics of the combustion and its prediction depends mainly in the use of chemical kinetics detailed mechanisms. These describe the elementary reactions that occur during a chemical process, foreseeing the consumption and destruction rates of all the intermediate species and products. Some of these kinetics mechanisms, mainly for long chain chemical species, such as isooctane, are formed by thousands of reactions which encloses hundreds of chemical species.

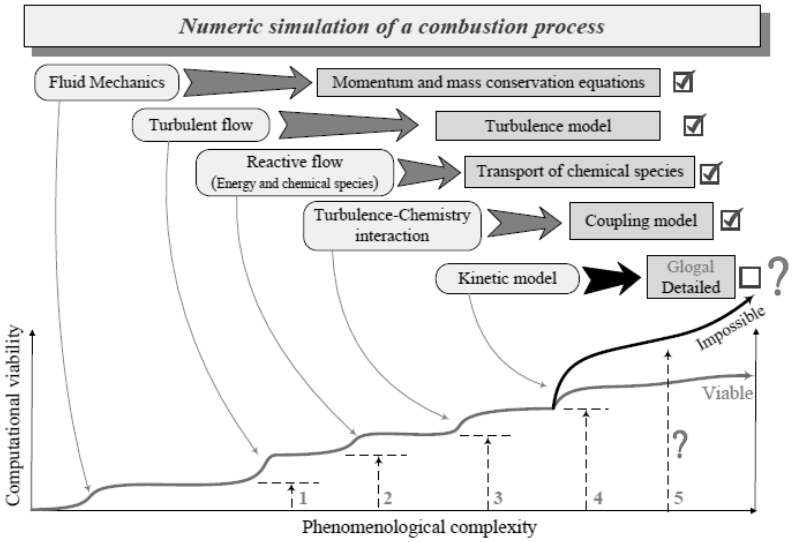

Figure 1 – Computational viability related to the phenomenological complexity in numerical simulation of a combustion process.
Source: Cancino, 2009.

From the numerical solution point of view, a three dimensional fluid dynamic problem requires the solution of a set of equation for the velocity and energy plus the mass conservation. The latter, in reactive problems, uses one equation for each species in the kinetics mechanism. More complex fuel kinetics mechanisms have thousands of species, which, in reactive problems, make it necessary to solve the same number of mass conservation equations. The growing of kinetics mechanisms rapidly increases the computational cost.

Cancino (2009) provides a graphic representation of the evolution of the computation effort with the increase in the complexity of the model. This diagram is reproduced in Figure 1. Usually, it is hardly feasible to use huge detailed kinetics mechanisms to the assessment and development of new technologies, and, for some applications, there is even no need for such model accuracy. However, several process and systems for kinetic combustion control, such as in HCCI, require more detailed data, but formatted in a way that a product may still be developed in a commercial time frame. In this sense, reduced mechanisms are useful for computational applications in product design and analysis.

A reduced mechanism is a group of species and reactions which represent a fraction of a detailed mechanism. They are obtained from the detailed mechanism using several distinct methods, such as sensitivity analysis (SA) or directed relation graph (DRG), under fixed thermodynamic conditions which describe a set of experiments and, therefore, are able to reproduce a given parameter. The usual target parameters are either local parameters, such as the temperature or a given species concentration, or global parameters, such as the laminar flame speed and the ignition delay time. There are several methods of performing the reduction, as it will be seen in Chapter 2. The analysis and synthesis of reduced mechanisms, applied for ethanol combustion, is the focus of this work.

Measurements of laminar flame speed, ignition delay time and concentration of species in perfectly-stirred reactors available in the literature were used as targets for the reduction. The reduction methods selected were the Sensitivity Analysis (SA), Rate of Production (ROP), Directed Relation Graph (DRG), Directed Relation Graph with Error Propagation (DRGEP), and Path Flux Analysis (PFA). The base detailed mechanisms selected were those of Leplat et al. (2011), from ICARE, Orleans, France, containing 252 reversible chemical reactions among 38 chemical species, developed mainly to reproduce measurements of species concentration in perfectly-stirred reactors; of Mittal et al. (2014),

from C3-NUI, Ireland, involving 710 reversible chemical reactions among 111 chemical species, developed mainly to predict ignition delay time measured in rapid compression machine; and that of Cancino et al. (2010), from IVG, Germany, and UFSC, Brazil, involving 1349 reversible chemical reactions among 135 chemical species, mainly developed to predict high pressure ignition delay time measured in shock tubes.

1.2. Objectives

1.2.1. General Objective

The main objective of this work is to generate reduced chemical kinetics mechanisms for the combustion of ethanol with air, under limited acceptable error bounds, at the conditions of temperature, pressure and equivalence ratio commonly found in the normal operation of spark ignited internal combustion engines.

1.2.2. Specific Objectives

In order to achieve the general objective, some specific goals are proposed:

1. To evaluate the selected ethanol detailed kinetics mechanisms to be used as bases for the reduction process;
2. To evaluate the different reduction methods taking into account the type and data needed by each of them;
3. To reduce the detailed mechanisms and to evaluate the final reduced mechanisms;
4. To analyze the efficiency and ease of application of the different methods;
5. To draw recommendations on the selection of a reduced mechanism for ethanol-air combustion applications.

1.3. Outline of the document

This document is divided in five chapters. Chapter 1 presents the introduction, including the motivations, boundaries and objectives. Chapter 2 presents the fundamentals and a review of the state of the art on the subject. This chapter covers concepts of chemical kinetics for combustion, the numerical treatment of chemical kinetics problems in

combustion, as well as the main reducing techniques currently used. The available detailed chemical kinetics mechanisms for combustion of ethanol and air are also reviewed. Chapter 3 presents the methodology adopted in this study. Chapter 4 presents the reduced mechanism obtained for the different strategies employed, as well as the comparison between the methods. Chapter 5 presents the main conclusions, recommendations for future work and is followed by the list of references.

2. LITERATURE REVIEW

The literature review covers the basics of the modeling of combustion processes using macroscopic conservation equations, the need and structure of detailed chemical reaction mechanisms, the basic experiments used for the development of chemical kinetics mechanisms for combustion, and the most used reduction methods.

2.1. Transport Equations for Reactive Flows

The modeling of chemical reacting flows under the hypothesis of the continuum demands the solution of a set of conservation equations for the mixture mass, momentum, and energy, as well as, the mass of chemical species. The chemical kinetics mechanism is a set of non-linear algebraic equations that describe the rate of transformation of reactants to products along the flow. These rates of reaction are strongly non-linear functions of the temperature, concentrations of chemical species and pressure. The chemical reaction rates, by their turn, change the mass of the chemical species and the sensible energy of the mixture. Therefore, the set of equations become strongly coupled and their solution gives rise to the presence of flame fronts and detonations.

The development of the complete set of conservation equations for reactive flows is presented by several authors (e.g., see review by Cancino, 2009). The conservation equations for the reactive flow of Newtonian fluids may be summarized in indicial notation as:

Conservation of Mass:

$$\frac{\partial \rho}{\partial t} + \frac{\partial}{\partial x_i} \rho u_i = 0 \,, \tag{1}$$

Conservation of Momentum:

$$\frac{\partial}{\partial t} \rho u_j + \frac{\partial}{\partial x_i} \rho u_i u_j = -\frac{\partial p}{\partial x_j} + \frac{\partial \tau_{ij}}{\partial x_i} + \rho \sum_{k=1}^{N} Y_k f_{k,j} \,, \tag{2}$$

$$\tau_{ij} = -\frac{2}{3} \mu \frac{\partial u_k}{\partial x_k} \delta_{\mathrm{ij}} + \mu \left(\frac{\partial u_i}{\partial x_j} + \frac{\partial u_j}{\partial x_i} \right), \tag{3}$$

Conservation of Energy:

$$\frac{\partial}{\partial t}\rho h + \frac{\partial}{\partial x_i}\rho u_i h = \frac{Dp}{Dt} - \frac{\partial q_i}{\partial x_i} + \tau_{ij}\frac{\partial u_i}{\partial x_j} + \dot{Q} + \rho\sum_{k=1}^{N} Y_k f_{k,i} V_{k,i}\,, \qquad (4)$$

$$q_i = -\lambda\frac{\partial T}{\partial x_i} + \rho\sum_{k=1}^{N} h_k Y_k V_{k,i}\,, \qquad (5)$$

Conservation of the mass of chemical species k:

$$\frac{\partial}{\partial t}\rho Y_k + \frac{\partial}{\partial x_i}\rho u_i Y_k = -\frac{\partial}{\partial x_i}\rho Y_k V_{k,i} + \dot{\omega}_k \quad , k = 1, \dots, N\,, \qquad (6)$$

$$\rho Y_k V_{k,i} = -\rho D_k\frac{\partial Y_k}{\partial x_i} - D_T\frac{\partial \ln(T)}{\partial x_i}\,. \qquad (7)$$

In these equations, $V_{k,j}$ represents the diffusion velocity, that was modeled above by Fick´s Law assuming that mass diffusion occurs as a result of gradient of mass fraction Y_k and temperature; $f_{k,i}$ denote the body force f acting on species k along the direction i; $\dot{Q}$ is the term representing the energy generation in volumetric units by others mechanism not related to combustion or phase change; q_i is the conduction heat transfer flux (modeled by Fourier's Law); τ_{ij} is the viscous stress tensor for a Newtonian fluid; Dp/Dt is the material derivate of the pressure; λ is the thermal conductivity of the mixture; D_k is the molecular mass diffusivity of species k in the mixture; D_T is the thermal mass diffusivity; ρ is the density; u_i represents the component i of the velocity vector u; h is the enthalpy; μ is the dynamic viscosity, and $\dot{\omega}_k$ represents the chemical reaction rate of species k calculated using the chemical kinetics mechanism (Cancino, 2009).

The chemical reaction rates are defined from a chemical reaction mechanism. In general, the higher the complexity of the chemical reaction mechanism in terms of number of species and reactions, the higher the accuracy in predicting the rates of change of the mass of chemical species. However, as a consequence, the larger becomes the computational effort needed to calculate a combustion problem. Therefore, as a way of reaching a compromise between computational time and accuracy, reaction mechanisms of different sizes

and complexities are available. In the following, the modeling of chemical reactions is reviewed.

2.2. Chemical Kinetics

2.2.1. Global Reactions

A global reaction is defined as a reaction involving one mole of oxidant with one mole of fuel, resulting in *n* moles of products and can be express generally as

$$F + aOx \rightarrow nPr \tag{8}$$

where *F* refers to one unit of fuel (in molar basis), *Ox* to one unit of oxidant, *Pr* to one unit of products, *a* and *n* are the stoichiometric coefficients, representing the amount of moles needed to achieve complete conversion of the fuel.

A global reaction kinetics is a semi-empirical expression that predicts the rate of change of the mass of species *k*. Usually, some sort of dependence on the concentration of reactants is assumed and the effect of temperature is accounted for in a rate constant. A common form of expressing a global reaction rate is

$$\frac{d[X_F]}{dt} = -k_G(T)[Fuel]^n[Oxidant]^m \tag{9}$$

where $[Fuel]$ and $[Oxidant]$ represent the molar concentration of fuel and oxidant respectively.

The property k_G is the apparent rate and is strongly dependent on temperature. The exponents *m* and *n* define the reaction order. They are empirically fitted to predict measurements of combustion characteristics, such as laminar flame speeds. Therefore, not needing to be integers and may even be negative numbers (Warnatz at al., 2010; Turns 2013).

The use of global reactions to model chemical kinetics is a simplification of a complex behavior and has found its usefulness in the solution of engineering problems where the rates of transport determine the outcome of the process. However, the use of global reactions does not provide a solid ground for understanding the details of the reaction process or to determine reaction controlled phenomena, such as ignition, extinction and some regimes of flame propagation. It is naive to think

that exactly n molecules of fuel would collide simultaneously with m molecules of oxidant, producing the final products in a single event of rearrangement of chemical bonds. What is known to occur is a chain of series and parallel elementary reactions often involving thousands of stable or excited chemical species, known as intermediates. Due to that fact, the approach to describe a chemical process involves the determination of the nature of the intermediate species and how they interact with each other in the form of elementary reactions.

2.2.2. Elementary Reactions

An elementary reaction is a one-step reaction that occurs molecularly in exactly the same way it is expressed by its equation. In an elementary reaction, the reactants form the products through a single transition state, without the presence of intermediate species. The overall reaction in fact occurs through a sequence of elementary steps. This approach presents several advantages as the fact that the reaction orders will always be integers and constants, independently of time and conditions.

The reaction molecularity is defined as the number of species that collide to form the activated complex. Only collisions among one, two and three species are statistically possible and they are named unimolecular, bimolecular and termolecular reactions.

Unimolecular reactions describe the dissociation or rearrangement of a single molecule. They are of order one and can be generically represented as

$$A \rightarrow products \tag{10}$$

Bimolecular reactions are the most common elementary reactions. They are of order two and can be generically represented as

$$A + B \rightarrow products \tag{11}$$
$$A + A \rightarrow products \tag{12}$$

Termolecular reactions are generally reactions of recombination and follow a third order behavior. They can be generically represented as

$$A + B + C \rightarrow products \tag{13}$$

$$A + A + B \rightarrow products \quad (14)$$
$$A + A + A \rightarrow products \quad (15)$$

The *Law of Mass Action*, that rigorously applies only to elementary reactions, states that the rate of reaction is proportional to the number of molecules of species appearing as reactants. From the Law of Mass Action, the rate of the bimolecular reaction

$$A + B \rightarrow C + D \quad (16)$$

is expressed as

$$\frac{d[A]}{dt} = -k[A][B]. \quad (17)$$

where k is the rate constant and $[I]$ is the molar concentration of species I.

In the same way that a collision between *A* and *B* can produce *C* and *D*, *A* and *B* can be formed from collisions of *C* and *D*. Therefore, in general a reaction can occur following both directions.

To describe that, two definitions are employed. The first choice uses two different reactions, that can only occur in one direction, the consumption of the reactants to form products. The second choice is to use two kinetic constants, a forward and a reverse kinetic constant. For the bimolecular reaction above, one could write

$$A + B \leftrightarrow C + D \quad (18)$$

In this case, the rate of production of *A* by the forward and backward reactions can be expressed, respectively, as

$$\left(\frac{d[A]}{dt}\right)_{\mathrm{f}} = -k_f[A][B]; \left(\frac{d[A]}{dt}\right)_{\mathrm{b}} = k_b[C][D] \quad (19)$$

where k_f is the rate constant for the forward reaction and k_b is the rate constant for the reverse reaction.

Therefore, the total rate of production of *A* can be expressed as

$$\frac{d[A]}{dt} = \left(\frac{d[A]}{dt}\right)_{\mathrm{f}} + \left(\frac{d[A]}{dt}\right)_{\mathrm{b}} = -k_f[A][B] + k_b[C][D] \quad (20)$$

The equilibrium constant of the reaction relates the forward and backward constants

$$Q_c = \frac{[C]^c[D]^d}{[A]^a[B]^b} = K_{eq} = \frac{k_f}{k_b} \tag{21}$$

where the exponents refer to the stoichiometric coefficients of the reaction.

2.2.3. Reaction Rate for Elementary Reactions

The dependency of the rate constant with the temperature may be modeled using an Arrhenius relation in the form

$$k(T) = A \exp\left(\frac{-E_A}{R_u T}\right) \tag{22}$$

where A is the pre-exponential factor, E_A is the activation energy and R_u is the universal gas constant.

The activation energy can be defined as the energy required to reach the transition state, as represented in the energy diagram of Figure 2.

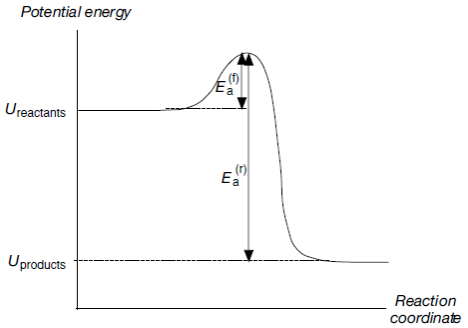

Figure 2 - Energy diagram for a chemical reaction
Source: Warnatz et al., 2010

The extended Arrhenius equation includes an additional dependency with temperature in the form

$$k(T) = A\,T^{b}\exp\left(\frac{-E_A}{R_u T}\right) \tag{23}$$

where *b* is the temperature exponent.

In some conditions, reaction rates may depend on the pressure as well. Two examples are the unimolecular reactions (or the recombination fall-off) and bimolecular reactions chemically activated. Generally, the reactions of the first kind have their rate increased when pressure increases, whereas reactions of the second kind behave in the other way. As a consequence, in general, recombination reactions on the limit of high pressure don't need a third body to absorb the energy after collision but in the lower pressure limit, for the reaction to occur, a third body is crucial. To address this dependency, some approaches were developed, as those proposed by Lindermann, Troe and Stewart. (ChemKin, 2009)

The Lindermann formula uses two distinctive coefficients for the rate, one for the lower limit and the other for the upper limit (k_∞ and k_0 respectively) being expressed as

$$k_0 = A_0 T^{\beta_0}\exp\left(-\frac{E_0}{R_u\,T}\right) \tag{24}$$

$$k_\infty = A_\infty T^{\beta\infty}\exp\left(-\frac{E_\infty}{R_u\,T}\right) \tag{25}$$

The rate constant is then interpolated using

$$k = k_\infty\left(\frac{P_r}{1+P_r}\right)F \tag{26}$$

$$P_r = \frac{k_0[M]}{k_\infty} \tag{27}$$

where *[M]* is the mixture molar concentration and P_r is the reduced pressure.

In the Lindermann approach, *F* is to unity. Troe suggested that *F* be evaluated from

$$\log F = log\ F_{cent}\left\{1+\left[\frac{\log P_r + c}{n - d(\log P_r + c)}\right]^2\right\}^{-1} \tag{28}$$

$$F_{cent} = a \exp\left(\frac{T}{T^*}\right) + exp\left(\frac{T}{T^{**}}\right) + (1-a)exp\left(\frac{T}{T^{***}}\right) \quad (29)$$

where $c = -0{,}4 - 0{,}67 \log F_{cent}$, $n = 0{,}75 - 1{,}27 \log F_{cent}$ and $d = 0{,}14$. In these expressions, T^*, T^{**}, T^{***} and a are empirical parameters.

The Stewart strategy evaluates F from

$$F = d\left[a \exp\left(-\frac{b}{T}\right) + \exp\left(-\frac{T}{c}\right)\right]^X T^e \quad (30)$$

$$X = \frac{1}{1 + (\log P_r)^2} \quad (31)$$

In this formulation, six parameters are necessary to calculate the lower and upper rate constant limits and the values of *a*, *b* and *c* are also needed. For the common reaction rate constant, using the extended Arrhenius formula, three parameters are required (*A*, *b* and E_a). For a pressure dependent reaction, three additional parameters are needed for the calculation of the higher and lower pressure limit rate constant. When the Troe formulation is used, three other parameters are needed, T^*, T^{**} and *a*, and T^{***} is optional. Similarly, if the Stewart strategy is employed, the values of three parameters (*a*, *b* and *c*) are required as well as the upper and lower rate constant parameters.

2.2.4. Treatment of Chemical Kinetic Mechanisms

As stated on section 2.2.1, a chemical process takes place through several steps, which can be described by elementary reactions. The set of all the elementary reactions among the chemical species that participate in a chemical reaction is defined as the chemical kinetics mechanism.

With the definition of reaction rate for elementary reactions presented on equations (24), (25) and (26), one can define mathematically the production/destruction net rates of any chemical species present in the mechanism. For example, consider the following set of reactions in the H_2-O_2 mechanism:

$$H_2 + O_2 \leftrightarrow HO_2 + H \quad \text{(R.1)}$$
$$H + O_2 \leftrightarrow OH + O \quad \text{(R.2)}$$
$$OH + H_2 \leftrightarrow H_2O + H \quad \text{(R.3)}$$
$$H + O_2 + M \leftrightarrow HO_2 + M \quad \text{(R.4)}$$

⋮

The net production of O_2 can be calculated as the sum of all the net production rates from all elementary reactions, i.e.,

$$\frac{d[O_2]}{dt} = k_{r1}[HO_2][H] + k_{r2}[OH][O] + k_{r4}[HO_2][M] + \cdots - k_{f1}[H_2][O_2] - k_{f2}[H][O_2] - k_{f4}[H][O_2][M] - \cdots \quad (32)$$

The terms with positive signs represent the formation of O_2 and those with negative signs account for its destruction. This analysis can be applied to all species present on the mechanism.

Due the fact that a kinetics mechanism can embrace several elementary reactions, a compact notation is employed. An elementary reaction can be represented generically as

$$\sum_{j=1}^{N} \nu'_{ij} X_j \leftrightarrow \sum_{j=1}^{N} \nu''_{ij} X_j \quad for \ i = 1,2,\dots,L \quad (33)$$

where ν'_{ij} and ν''_{ij} are the stoichiometric coefficients of the reactants and products respectively for species *j* on reaction *i*. This simplified notation allows the use of matrices (in fact, highly sparse matrices) to represent the mechanism, facilitating the numerical treatment.

The rate of reaction of reaction *j* is calculated from

$$\dot{\omega}_j = \sum_{i=1}^{L} \nu_{ij} q_i \quad for \ j = 1,2,\dots,N \quad (34)$$

where the shorter notation

$$\nu_{ij} = (\nu''_{ji} - \nu'_{ji}) \quad (35)$$

is used.

Then, the net rate of production of species *i* becomes

$$q_i = k_{fi} \prod_{j=1}^{N} [X_j]^{\nu'_{ji}} - k_{ri} \prod_{j=1}^{N} [X_j]^{\nu''_{ji}} \quad (36)$$

In the essence, in order to obtain a chemical kinetics mechanism for a process that takes a species *A* to produce *B*, in principle, all the possible combinations of species that can exist with the elements of *A* and *B* with all the reactions that may connect these species must be accounted for. The number of intermediate species could be so large that the size of the final mechanism would be too large, making it difficult to use it in the prediction of an engineering problem. However, the analysis of the mechanism usually reveals that several species have a very small impact on the whole process and some of them would even be statistically impossible to appear. Therefore, the experience of the modeler and several techniques have been applied to eliminate unimportant reactions and species and in such a way to make the mechanism smaller and simpler to be used. Smaller mechanisms demand less computational effort and require a smaller number of parameters.

The simpler mechanisms are named skeletal and reduced mechanisms. Skeletal mechanisms make extensive use of partial equilibrium and steady-state assumptions to achieve very small and robust chemical kinetics mechanism. Skeletal mechanisms may be expressed as set of complex rate equations due to the equilibrium and steady-state assumptions. Reduced mechanisms keep the basic structure and reaction paths of the detailed mechanism, but eliminate unimportant reactions and species. In order to be able to test the detailed and reduced mechanisms target experiments are needed.

2.3. Typical Experiments for Chemical Kinetics

The basic description of the experiments and references can be found in Cancino (2009), among others

2.3.1. Constant Volume Reactor (CVR) or Batch Reactor

The constant-volume reactor is the simpler configuration of a chemical reactor. It consists in a closed vessel where the reactants are admitted and blended. The reaction takes place in this confined space and pressure and/or temperature are measured along the reaction time. Species concentration measurement can also be performed. The main hypothesis behind the static reactor is the fact that the mixture is homogeneous, presenting no gradients of temperature or pressure in all domain.

When a flame develops after a central ignition, the flame surface position can be recorded as a function of time. Usually, the extraction of meaningful data requires the numerical treatment of the measurements following a set of simplified assumptions regarding the flame thickness and the effect of flame stretching. The reactor can also be operated under turbulent flow conditions by the use of fans to stir the mixture.

2.3.2. Plug-Flow Reactor (PFR)

The plug flow reactor (PFR) uses a uniform flow within a tube to ensure an area-averaged homogeneous mixture and to set the desired range of residence time along the tube. Generally the mixture is highly diluted by inert gas in order the set the reactor temperature and pressure independent of the reaction rate. The reaction zone, in this type of reactor, extends for a long distance across the tube and the diffusive effects are neglected when compared to convective effects. Since the mixture properties are constant along the tube, the one-dimensional problem can be converted to a zero-dimensional problem (only dependent on time).

In this reactor, usually the mixture oxidant-fuel ratio, temperature, pressure, presence of diluents and flow rate are set. The species concentrations are measured at different positions along the tube, allowing for sampling at different residence times during the same run.

2.3.3. Perfect Stirred Reactors (PSR) or Continuous Stirred-Tank Reactor (CSTR)

The perfectly-stirred reactor (PSR) uses a high-speed flow to ensure a homogeneous mixture and to set the desired residence time of the mixture within a short reactor. Generally the mixture is highly diluted in inert gas in order the set the reactor temperature and pressure independent of the reaction rate. In the ideal reactor, the mixing of reactants and products is almost perfect, resulting in very small thermal gradients and the diffusive effects are neglected. Then, the problem can be treated as a zero-dimensional problem (time dependent). The Jet Stirred Reactor (JSR) is the closest approximation to a perfectly stirred.

In this reactor, usually the mixture oxidant-fuel ratio, temperature, pressure, presence of diluents and residence time are set. The species concentrations at the outlet of the reactor are measured. The

experiment can also be used to assess ignition, extinguishment and the presence of negative temperature coefficient (NTC) region.

2.3.4. Shock Tube (ST)

The shock tube experiment (ST) employs a planar shock wave that compresses a mixture of reactants untill the pressure and temperature desired are achieved. The ignition delay time (IDT) is defined as the time interval between the arrival of the wave and the start of combustion. The composition, temperature and pressure of the driver gas is tailored to achieve the final temperature and pressure of the driven gas. Combustion can be detected from the transient measurement of the pressure within the reactor or from the spontaneous emission or absorption of intermediate species, such as OH and CO.

Usually, the return is the ignition delay time (IDT) as a function of stoichiometry, temperature and pressure. The technique is normally applied for medium to high pressure, medium to high temperature and relatively high saturation vapor pressure fuels. There are experiments developed to work directly with fuel sprays. Negative temperature coefficient region can be detected.

2.3.5. Rapid Compression Machine (RCM)

The main focus of a rapid compression machine is to emulate the process of compression that takes place on internal combustion engines. In this type of experiment, the mixture located in a combustion chamber undergoes a fast volumetric compression generated by the motion of a piston. The increase in the pressure and temperature triggers thermal ignition. The compression ratio, initial pressure and mixture composition can be varied to control the pressure and temperature values after combustion.

This experiment is applied from low to medium pressures and temperatures relatively smaller than those achieved by shock tubes. The reliability of the results depends on the proper modeling of the compression and ignition of the mixture. The longer the ignition delay, the stronger are the effects of heat transfer to the wall in the state of the mixture. Experimental measures are also taken to minimize the entrainment of mixture from the boundary layer into the core mixture, as well as, to minimize losses of mass across the piston-cylinder clearance (blow-by) (Sung and Curran, 2015).

2.3.6. Laminar Flat-Burner (LFB)

The laminar flat-burner (LFB) is intended to allow for stabilization and probing of a laminar flat flame as a mean to study a reactive system where both chemical kinetics and diffusive processes determine the flame speed and structure.

The stabilization of laminar premixed flame is generally obtained by heat loss to a burner surface, which may be either porous or perforated. The experiment is designed either to minimize the heat loss or to work with a known amount of heat loss. The laminar flame speed is an overall parameter used to test detailed chemical kinetics mechanisms. Stoichiometry, temperature and pressure may be changed. The experiments are usually run at near ambient temperatures (ambient to 500 K) and pressure. Low pressure flames (sub-atmospheric) are used to enlarge the flame thickness and allow for detailed probing and measurement of species concentration along the flame front (Egolfopoulos et al., 2014).

2.4. Chemical Kinetics Mechanisms for Ethanol

The assembly of detailed chemical kinetics mechanisms for the oxidation of hydrocarbon follows a hierarchical structure, as presented in the diagram in Figure 3. The kinetics mechanism for the combustion of a higher hydrocarbon encompasses the mechanisms for the smaller hydrocarbons, aldehydes and finally the CO and H_2 oxidation mechanisms. The hierarquical structure allows that the sub-mechanisms be developed and tested separately before the interactions among sub-mechanism arise. Due to the interactions, any change to a sub mechanism needs to be tested against all the measurements available for all the fuels encompassed by the mechanism. The predictions are affected by the uncertainties in the kinetics parameters and are only accurate in that extent.

The development of mechanisms for ethanol followed the same principle. In the last 30 years several measurements of the oxidation of ethanol in the presence of nitrogen, carbon dioxide, water, nitrogen oxides and several other hydrocarbons and alcohols became available. Sarathy et al. (2014) present a thorough review of the measurements available. Based on these measurements, there have been many efforts to develop chemical reaction mechanisms. summarizes the more recent attempts.

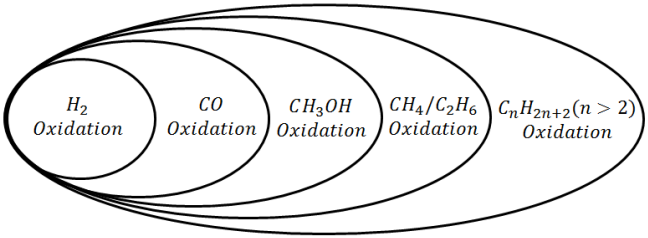

Figure 3 – Hierarchy of reactions in a mechanism describing the combustion of an aliphatic hydrocarbon
Source: Warnatz et al., 2010.

Earlier measurements and mechanisms were developed by Natarajan and Bhaskaran (1982) for IDT from shock tube; Gulder (1982) for laminar flame; Borisov et al. (1991) for pyrolysis; Dunphy et al. (1991), Dunphy and Simmie (1991) and Curran et al. (1992) for IDT from RCM; Egolfopoulos et al. (1992) for laminar premixed flame, flow reactor and shock tube; and Norton and Dryer (1992) for flow reactor.

Marinov (1999) reviewed the branching ratios for the three isomers obtained from the H abstraction from ethanol and also the rates of fuel pyrolysis. He tested his mechanism against a broad range of measurements, including laminar flame speed, ignition delay time, species concentrations from jet-stirred reactor and from counter flow burner.

Li (2004) developed a mechanism based on previous work by Norton and Dryer (1999) and updates from Marinov (1999). The mechanism was tested against measurements of species concentration in flow reactor.

Saxena and Williams (2007) started from the San Diego Mechanism for C1 and C2 hydrocarbons and added reactions from Li (2004). The peroxide species and reactions are removed, since the target was a high-temperature mechanism. The fall-off constants for ethanol pyrolysis were updated. Sub-mechanisms were tested for formaldehyde, methane, methanol, ethane, ethylene, acetylene, propane, and acetaldehyde. The ethanol mechanism was tested against ignition delay time from shock tube, laminar burning velocity, diffusion-flame extinction in a counter-flow burner and their respective concentrations of chemical species. Olm et al. (2015) optimizes the kinetic constants of Saxena and Williams (2007) mechanism using a "*n*" objective function

that takes into account the deviations for several targets, including ignition delay, laminar burning speed, and species concentrations from flow and jet-stirred reactors. They adjust the kinetics constants of 14 elementary reactions identified as the most sensitive in respect to the targets.

Rohl and Peters (2007) reduced the mechanism by Marinov (1999) in order to diminish the computational costs in numerical simulations. They decreased the number of species from 57 to 38 and the number of reactions from 288 to 228. Their predictions were tested against IDT measurements in shock tube and laminar flame velocities.

Cancino et al. (2010) published a model for the ethanol oxidation developed from the Konnov mechanism for C3 hydrocarbons and the Marinov mechanism for ethanol. Some elementary reactions and kinetic constants were reviewed based on Li (2004), Park et al. (2002), Park et al. (2003), and Xu et al. (2004). The model was validated against measurements of ignition delay time from shock tube experiments, for a stoichiometric mixture, at temperature of 750 K to 1200 K and a pressure range of 10 bar to 50 bar, and for a lean mixture at equivalency ratio of 0.3, at the same temperature range and pressure of 30 bar.

Orbegoso et al. (2011) performed a comparison among predictions and measurements of laminar flame speed, ignition delay time measured in shock tube and species concentration profiles from JSR with the predictions of the mechanisms by Egolfopoulos et al. (1992), Marinov (1999), Saxena and Williams (2007), Dagaut and Togbé (2008) and Cancino et al. (2009). They show that Cancino´s mechanism was not able to accurately predict chemical species measured in JSR at 1 and 10 bar. The best overall predictions were provided by Dagaut and Togbé (2008) whose mechanism was latter improved by Leplat et al (2011).

Leplat et al (2011) performed an experimental and numerical study of the oxidation of ethanol in laminar premixed flames in a jet stirred reactor (JSR). Dagaut and Togbé (2008) developed a mechanism for mixtures of gasoline and ethanol obtaining a structure with 1866 reactions among 235 species. Their sub-mechanism for ethanol upgraded Dagaut (2002) mechanism for natural gas with the reactions and constants from Marinov (1999). Leplat et al. (2011) upgraded the reaction constants, added a few reactions and proposed a detailed chemical kinetics mechanism with 252 reversible reactions among 38 species (including nitrogen and argon). They tested the mechanism against measurements of species concentration in the JSR, ignition delay

time in a shock tube, and species concentration in premixed, partially-premixed and nom premixed flames.

Demetrio (2011) compared the predictions of the mechanisms by Leplat et al.(2011), Cancino et al. (2009), Saxena and Williams (2007), Li et al. (2003) and Marinov (1999) against several measurements from shock tube (ST), rapid compression machine (RCM), counter-flow burner (CF) and flat-flame laminar burners. He found that the best overall predictions were provided by Leplat´s mechanism, even though Cancino´s mechanism had a better performance for the IDT measurements.

Tran et al (2013) developed mechanism starting from a base mechanism for C0 to C4 and adding the reactions of ethanol. The ethanol mechanism is divided in a primary and secondary mechanisms. In the primary mechanism six channels for decomposition of ethanol are considered. These channels form acetaldehyde, formaldehyde, ethenol and ethylene, which are the secondary mechanisms considered. The mechanism was tested against species measurements taken in a low pressure flat burner and then compared to laminar burning velocity.

Mittal et al. (2014) published a chemical kinetics mechanism for the oxidation of ethanol composed by 111 species and 710 reactions. This mechanism was an updated version from Dunphy et al (1991) which had 97 reactions and 30 species. They were tested against the IDT measured in shock tube by Dunphy and Simmie (1991), in the temperature range of 1080 K to 1660 K, pressure range from 1.8 bar to 4.6 bar and equivalency ratios from 0.25 to 2, and against their IDT measurements in RCM at 825 K to 985 K, pressure range from 10 bar to 50 bar and equivalency ratios from 0.3 to 1.0. The mechanism was also extensively tested against a wide range of initial conditions and experimental reactors named ST, JSR, FR, flame species and flame speed. They did not include the NO_x mechanism.

Herrmann et al. (2014) studied the low temperature oxidation of ethanol in an atmospheric pressure laminar flow reactor at equivalence ratios of 0.8, 1.0 and 1.2 and temperatures from 400 to 1200 K. They tested the mechanisms of Cancino et al. (2010) and Zhao et al. (2008). Zhao´s mechanism was developed for dimethyl-ether and can also be applied to ethanol. The ethanol sub-mechanism was tested against premixed flames, ignition delay and flow reactors.

Table 1 – Summary of studies that present and test chemical kinetics mechanisms for ethanol.

(continue)

Reference	Mechanism			Conditions tested			
	No. of species	No. of reactions	Characteristics	Experiment	Φ	T / K	p / bar
Dunphy et al (1991)	30	97	Based on a methanol oxidation mechanism	ST	0.25-2.0	1080-1660	1.6-4.6
Egolfopoulos et al. (1992)	35	195	Developed with C1, C2, CH_3OH and C_2H_5OH sub mechanisms	CF ST	0.6 – 1.8	363-453 1000-1700	1
Marinov (1999)	57	393	Differentiate all three distinct sites of hydrogen abstraction in the C_2H_5OH	CF ST JSR FR LBV	0.6-1.4 0.5-2.0 0.2-2.0	298-453 1300-1700 1000-1200	1-2 1-3.4 1
Alzueta and Hernandez (2002)	79	536	With NOx chemistry	FR	1,0	700-1500	1
Saxena and Williams (2007)	57	288	With NOx chemistry (14/53) and compounds with C3 (7/43)	LBV ST CF	1.0 0.25, 0.5, 1.0, 2	298 - 453 300 - 2000	1 1, 2

(continuation)

Cancino et al. (2010)	136	1136	Based on Marinov (1999) and Konnov (2005) models	ST	0.25-2.0	650-1600	2-50
Leplat (2011)	38	252	Based on Marinov (1999) and GRI mechanism with improvements for several conditions	JSR CF LBV ST	0.25,1.0, 2.0 0.75 - 1.25 0.7 – 1.5 0.5 – 2.0	448 300 - 453 1100 - 1500	1, 10 50 mbar 1 - 10 2 – 4.5
Tran et al. (2013)	87	760	Based on a mechanism for C0-C4	LPFB, O_2 + Ar diluted flame LBV	0.7, 1.0, 1.3 0.5-1.7	333 298, 358, 398, 453	6.7 kPa 1
Mittal et al. (2014)	111	710	Validated for low temperature and high pressure ethanol autoignition	ST JSR FR LBV CF	0.5 – 2 0.25-2 0.3 – 1.4 0.6 - 1.8	800-1760 890-1250 800-1100 298 - 453	2 – 40 1 3-12 1-8

Legend:
IDT – Ignition delay time, LBV – Laminar Burning Velocity, CF- Counter-Flow Burner, FR – Flow Reactor, JSR - Jet-Stirred Reactor, ST - Shock tube, LPFB - Low Pressure Flat Burner.

Both mechanisms are shown to reproduce the species measured in the flow reactor.

The analysis of the available mechanisms led to the choice of the mechanisms that will be reduced. The analysis of reaction paths will be presented in the chapter on results.

2.5. Reduction Methods for Kinetics Mechanisms

Reduced mechanisms are very useful in numerical simulation of combustion processes. It this sense, one can identify two uses of reduced mechanisms. The first is the use of a dynamic mechanism, which uses a different kinetics mechanism for each simulation step (space and/or time), whose reduction is obtained directly for the local conditions found on that time or spatial step. The second use, namely, the use of a static mechanism, produces a reduced mechanism from a set of targets which is used for every step in the subsequent simulations and is basically independent of the problem and the solver. This work focus on static mechanisms.

Several approaches are employed for the reduction of kinetics mechanisms using static reduced mechanisms. The main methods are named:

- QSSA – Quasi-Steady State Analysis;
- PE – Partial Equilibrium;
- PCA – Principal Component Analysis;
- CSP – Computational Singular Perturbation;
- ILDM – Intrinsic Low-Dimensional Manifold;
- SA – Sensitivity Analysis, which includes the Direct Sensitivity Analysis (DSA) and Normalized Direct Sensitivity Analysis (NDSA);
- ROP – Rate of Production;
- DRG – Directed Relation Graph;
- DREP – Directed Relation Graph with Error Propagation;
- DRGEPSA – Directed Relation Graph with Error Propagation aided Sensitivity Analysis;
- PFA – Path Flux Analysis;
- RFA – Reactivity Flux Analysis;
- FPT – Flux Projection Tree;
- GA – Genetic Algorithms.

Table 2 presents a summary of a few authors and the methods studied.

Table 2 - Authors and the reduction techniques used.

Author	**Year**	**Method(s)**
Lu and Law	2005	DRG; DRG + CSP
	2006	DRG
Hernández et al.	2010	GA
Niemeyer et al.	2010	DRGEPSA
Okuyama et al.	2010	QSSA
Shi et al.	2010	DRGEP + PCA
Sun et al.	2010	PFA
Demetrio	2011	DSA
Tosatto et al.	2011	Path flux DRG
	2013	DRG based methods
Bahlouli et al.	2012	DRGEP + CSP
Karadeniz	2012	DSA + RFA
Zhang et al.	2013	QSSA + PFA
Bahlouli et al.	2014	DRGEP + PCA
Liu et al	2014	FPT

2.5.1. Quasi-Steady State (QSS) and Partial Equilibrium (PE)

On reactive problems, frequently, there are intermediate species that present a behavior that can be approximated as a steady state. This occurs when the concentration of a given species is nearly constant, having the production rate almost equal to the consumption rate. This is the behavior exhibited by species S2 on Figure 4, an example taken from Warnatz et al. (2010).

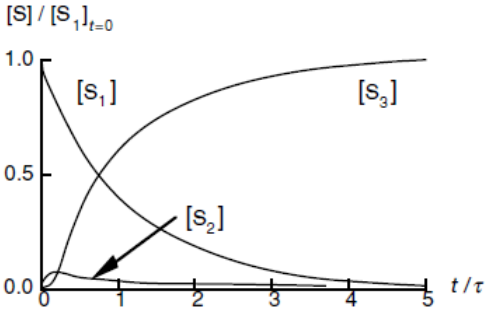

Figure 4 – Variation with time of the non-dimensional concentration of the chemical species S_1, S_2 and S_3 that participate in the simple chain reaction mechanism expressed as $S_1 \rightarrow S_2 \rightarrow S_3$
Source: Warnatz et al., 2010.

This behavior is more common for radicals, which are very reactive species. When this behavior is identified, a steady state simplification can be used.

$$\frac{d[X_j]}{dt} = \dot{\omega}_j = \sum_{i=1}^{L} \nu_{ij} q_i = 0 \,. \tag{37}$$

This removes the differential equation for the species flagged as in QSS from the set of mass conservation equations and replaces it by an algebraic equation, thus reducing the effort to solve the reactive problem.

The downsizes of this approach is that, sometimes, the algebraic equation used for calculating the concentration of the QSS species becomes too complex, which can slow the solver instead of speeding it up. Also, it may need an adjustment on the combustion solver as the QSS species will have a separate equation to be used for it.

This type of reduction strategy involves the identification of the QSS. Methods, such as the Computational Singular Perturbation (CSP) or the Intrinsic Low-Dimensional Manifold (ILDM) were developed to separate species on fast and slow-changing domains and therefore identify the QSS species.

The main idea of CSP is to find the reactions that evolve in the fastest time-scales based on a timescale analysis of the Jacobian matrix. When the contribution of these reactions become too small, they can be

decoupled from the system, reducing the stiffness of the system of ODEs. More details about this method can be found on Lam and Goussis (1988).

The Intrinsic Low Dimensional Manifold (ILDM) is another method based on QSS, although the main goal is not to reduce the stiffness of the ODE system but instead to reduce the state space of reactions systems so that it can be tabulated for subsequent use. The method was presented by Maas and Pope (1992) and more in-depth information can be found on their work.

2.5.2. Sensitivity Analysis (SA)

The rate laws for a mechanism consisting of *R* reactions among *S* species can be represented as,

$$\frac{d[X_i]}{dt} = F_i([X_1], \dots, [X_S]; k_1, \dots, k_R)$$
$$[X_i](t = t_0) = [X_i]^0 \qquad i = 1,2, \dots, S \tag{38}$$

where c_i is the molar concentration of species i, the dependent variable, t is the time, the independent variable, and k_r denotes the parameters of the system.

The dependence of the solution $[X_i]$ on the parameters k_r is called sensitivity. The absolute and relative sensitivities can be defined, respectively, as

$$E_{i,r} = \frac{\partial [X_i]}{\partial k_r}, \tag{39}$$

$$E_{i,r}^{rel} = \frac{k_r}{[X_i]} \frac{\partial [X_i]}{\partial k_r} = \frac{\partial \ \ln [X_i]}{\partial \ln k_r}. \tag{40}$$

Generally, an analytical solution of the sensitivity differential equations is not possible, but they can be solved numerically. By differentiating the equation (38), one obtains (Warnatz et al., 2010)

$$\frac{\partial}{\partial t} E_{i,r} = \left(\frac{\partial F_i}{\partial k_r}\right)_{c_l, k_{l \neq r}} + \sum_{n=1}^{S} \left\{ \left(\frac{\partial F_i}{\partial [X_n]}\right)_{[X]_{l \neq n}, k_l} E_{n,r} \right\} \tag{41}$$

The Jacobian matrix is defined as

$$J_{il} = \frac{\partial F_i}{\partial [X_l]} \tag{42}$$

Equation (41) is solved by numeric integration to obtain the sensitivity of $[X_i](t)$ on k_r (Cancino, 2009). Other target variables can also be chosen for the sensitivity analysis.

Several studies using direct sensitivity analysis (DSA) and normalized direct sensitivity analysis (NDSA) for optimizing reaction rate coefficients were performed. This analysis can identify the most sensitive reactions for the variable chosen as target, e.g., the temperature, the mass fraction of a given species, or the laminar flame speed. Figure 5 presents a typical sensitivity diagram.

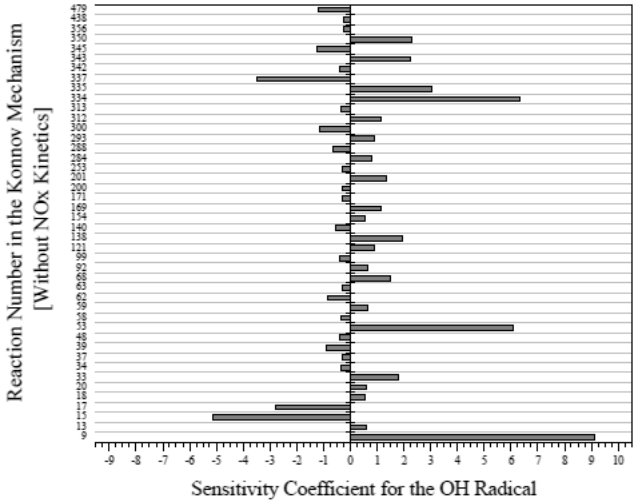

Figure 5 - Typical bar diagram generated from a sensitivity analysis at a specific elapsed time during the ignition delay in a shock tube.
Source: Cancino, 2009.

The reactions with very small sensitivity coefficients can be removed from the mechanism with a negligible effect.

2.5.3. Reaction Rate Analysis

All methods in this category require only the knowledge of the solution of the kinetics equations to identify which reactions and species are not determining of the outcome of the reaction process. The main goal of these methods is to identify how each species and reaction is coupled and, then, to quantify the importance of these connections.

2.5.3.1. Rate of Production (ROP)

The goal of the Rate of Production (ROP) method is to remove elementary reactions whose contribution to the formation and consumption of the species is so small that they can be ignored. The ROP index is used to quantify the fraction of production/consumption that each reaction contributes in the rate of formation/destruction of each species (Warnatz et al., 2010). Table 3 presents an example of a table of ROP indices calculated from a hypothetical chemical reaction mechanism.

Table 3 – Example of a ROP index table.

	Species				
	1 (%)	**2 (%)**	**…**	**n-1 (%)**	**n (%)**
Reaction 1	1	15	…	0	72
Reaction 2	0	1	…	0	2
⋮	⋮	⋮	⋮	⋮	⋮
Reaction m-1	0	0	…	10	25
Reaction m	5	0	…	2	1
Total	100	100	…	100	100

In the example presented in Table 3, 72 % of consumption/formation of species N can be related to reaction 1, 2 % to reaction 2, 25 % to reaction m-1 and 1 % to reaction m. Each row

represents the fraction of the reaction contribution to consumption/formation of each species. Small values over an entire row means that the reaction correspondent to that row has a small importance for the chemical process. In the other hand, a high value on a row means that the reaction on analysis is important for at least one species. Reactions that the maximum value over the entire set of species present a small value, e.g. 1 %, can therefore be removed from the mechanism since its contribution to the mechanism is negligible.

The method can be applied globally or locally, with respect to the species that participate in the reaction mechanism. The global approach is applied over all species. When the ROP index of a reaction is smaller than a user-defined limit, the reaction is removed from the mechanism. The global approach does not result in the removal of species because when a species participates in a small number of reactions, their ROP index becomes very large. The local approach applies the method for only a partial list of species. Any reactions that involve the important species and whose ROP index is smaller than the limit are removed. In the end, the reduced mechanism is composed by all the remaining reactions and the species involved on them.

These indexes can be either obtained using the net reaction rate or forming two tables, one composed by only consumption data and other only by production. Lebedev (2010) presents the ROP index of the reaction *j* related to species *i* as the ratio of the fraction of the net production of the reaction *j* over the total net production of the species *i*,

$$I_{ij} = \frac{\nu_{ij}(|\omega_{f,j}| + |\omega_{r,j}|)}{\sum_k \nu_{ik}(|\omega_{f,k}| + |\omega_{r,k}|)} \tag{43}$$

where $\omega_{f,j}$ represent the forward reaction rate of reaction *j* and $\omega_{r,j}$ is the reverse reaction rate.

2.5.3.2. Directed Relation Graph (DRG)

According to Lu and Law (2005), experience has shown that it is simpler to remove unimportant reactions than. Each species is linked to the formation of others, both directly, or through a sequence of formation/destruction of other intermediates. This link may be strong, for example, when both species are related directly in a fast reaction or indirectly via a third species. Therefore, the removal of a species from a mechanism brings the consequence of needing to remove all the other

species strongly coupled to it. In the same way, the inclusion of a species in a mechanism requires that all species with strong connections to it must be added as well.

The directed relation graph (DRG) method is one of many methods to quantify the level of the connection between two species and therefore evaluate its importance. This method requires the knowledge of the production rate of a species *A*, given as

$$R_A = \sum_{i=1}^{I} \nu_{A,i}\omega_i \,, \tag{44}$$

where the net production rate is

$$\omega_i = \omega_{f,i} - \omega_{b,i} \tag{45}$$

The importance index quantifies the influence of a species *B* in the production/consumption of *A*. The importance index of *A* in respect to *B* is defined as

$$I_{AB} = \frac{\sum_{i=1,I} |\nu_{A,i}\omega_i\delta_{Bi}|}{\sum_{i=1,I} |\nu_{A,i}\omega_i|} \tag{46}$$

$$\delta_B^i = \begin{cases} 1\,, & if\ \upsilon_{B,i} \neq 0 \\ 0\,, & if\ \upsilon_{B,i} = 0 \end{cases} \tag{47}$$

where *I* is related to the number of reactions in the mechanism.

Then, the importance index for species *B* is defined as

$$I_B = \max_A (I_{AB}) \tag{48}$$

The criteria for elimination of species *B* is evaluated by

$$I_B = \begin{cases} \geq \varepsilon\,, add\ B\ to\ \Omega \\ < \varepsilon\,, B\ is\ not\ important \end{cases} \tag{49}$$

where ε is the user threshold and Ω is the important species list.

If I_B is greater than the threshold, the absence of species *B* would inflict a greater relative error on the mechanism. For example, if a species *B* with an index of 0.3 relative to *A* is removed, this action is expected to cause a maximum error of 30 % when calculating the

concentration of *A*. Therefore, the definition of the threshold is important for the success of the method.

An example of how DRG works can be observed on Figure 6. The method operates in a progressive way, from a starting point (an important species list), adding species and reactions until reaching the limit imposed by the threshold. The species in evidence in the diagram are the ones that are progressively added to the final mechanism, i.e., the reduced mechanism. The arrows represent the relation among each species and the thickness of the arrow represents the magnitude of this relation. The process starts in diagram (a), where only species *A* is in the reduced mechanism. In the next step, shown in diagram (b), only species *C*, *D* and *F* have the index greater than the limit and therefore, they are included in the reduced mechanism. At (c), with the presence of species *C*, *D*, and *E* as part of the mechanism, more species become important and are added. The process follows to (d) and finally reaches the reduced mechanism presented in (e). We notice that species *B*, *E*, *G* and *H* never made to the final mechanism because their indices never overcame the threshold. In this method, a graph of the mechanism can be build, taking each species as a vertex and the connection between them as the importance index. In the final reduced mechanism there will be a connection between two species *A* and *B* only if the index I_{AB} is greater than the threshold. All the species that do not have a link to the important list are therefore removed from the mechanism as well all the reactions that may involve them.

Lu and Law (2005) started from a detailed mechanism consisting of 70 species and 463 elementary reactions for the combustion of propane. Using DRG and measurements from PSR and IDT as targets, they developed a reduced mechanism for the combustion of ethylene with 33 species and 205 reactions. They observed that even smaller mechanisms could be achieved when the threshold was increased or by reducing the domain of target points utilized for the reduction. However, the additional reduction paid the price of loss of accuracy and comprehensiveness. Employing a CSP method, a skeletal mechanism was obtained by further reducing the 33 species mechanisms. The final reduced mechanism obtained consists of 20 species and 16 semi-global reactions. Both mechanisms presented a high fidelity compared to the detailed one.

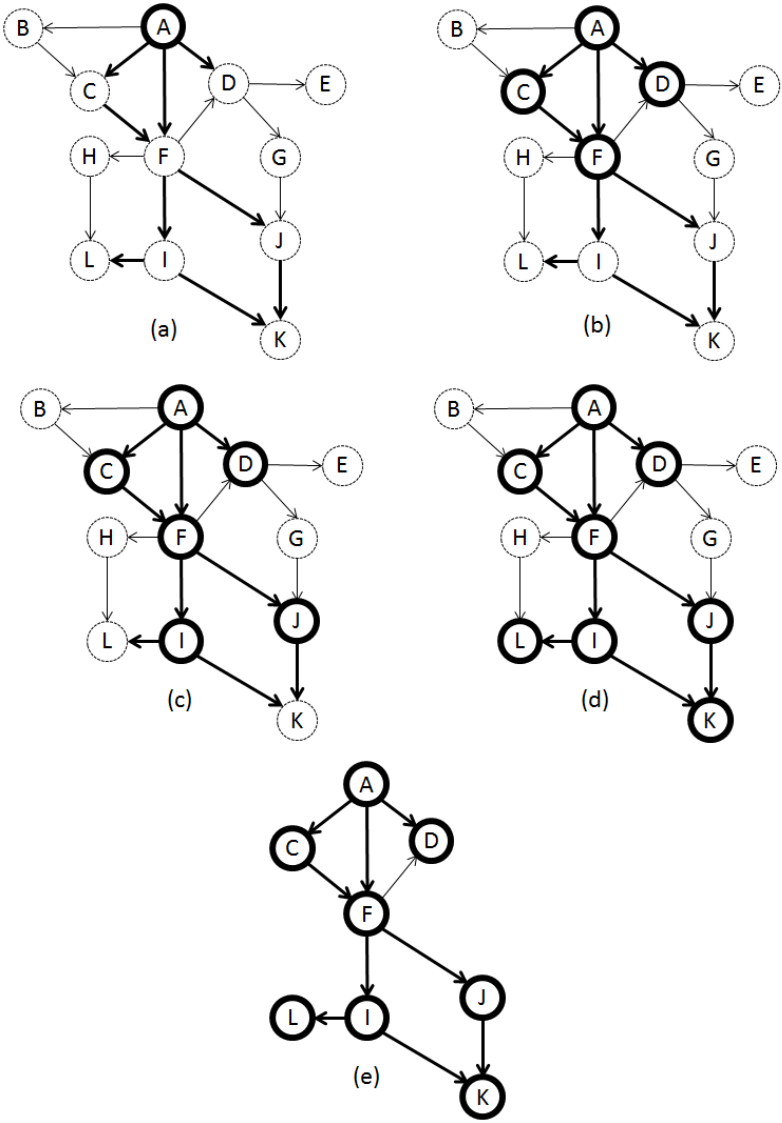

Figure 6 – Example of DRG progression. (a) Initial Mechanism starting with species A as important; (b), (c) and (d) represent the progression of the method; (e) Final reduced Mechanism.

In the same study, a sample with 1000 data points in the conditions of pressure from 0.1 atm to 30 atm, equivalency ratios from 0.7 to 1.3, temperature of 300 K (for the PSR) and from 1000 K to 1800 K (IDT) were used. However, they observed that a much smaller sampling would be adequate for the specified accuracy.

In the sequence, Lu and Law (2006a) used a two-stage reduction strategy employing DRG to reduce n-heptane (561 species) and iso-octane (857 species) detailed mechanisms using data from PSR. The final mechanisms are composed by 188 and 233 species respectively. They showed that after the first stage, the graph structure is modified and some moderately important species may become unimportant for the main reaction path way. Therefore, the second stage aims at identifying these species and removing them from the final mechanism.

On another study, Lu and Law (2006b) evaluated the applicability of the DRG method when coupled to several other methodologies, such as QSS, PE, DRG with dormant modes, and DRG with error propagation (DRGEP). They concluded that the reduction time for large mechanisms was linearly proportional to the number of reactions in the mechanism. Also, the method requires minimal system knowledge and can be fully automated, which makes this process suitable for case-specific and also for dynamic reductions.

Tosatto, Bennett and Smooke (2012) studied the use of DRG in six different configurations (using the index forms proposed by Lu and Law (2005), Pepiot-Desjardins and Pitsch (2008) and Luo et al. (2010) in the DRG and DRGEP formats) to reduce a two-component surrogate for JP-8 jet fuel (composed by 234 species and 6997 reactions). The data sources include adiabatic ignition with initial temperature of 1000 K and a PSR with inlet temperature of 500 K. The pressure range varies from 1 to 40 bar and the equivalency ratio from 0.5 to 2. The maximum deviation allowed from the solution was 5 % between the reduced and the detailed mechanism. The number of species in the final mechanism obtained spans from 127 to 150 for the DRG and 124 to 136 for the DRGEP strategies.

2.5.3.3. Directed Relation Graph with Error Propagation (DRGEP)

The Directed Relation Graph with Error Propagation (DRGEP) is an extension of the DRG method. This method employs a strategy that takes into account the distance of a species *B* to species *A* (on the

important species list) to evaluate the importance index. Lebedev (2010) suggests the following importance index:

$$I_{AB} = \frac{\sum_{j=1,I} \left| \nu_{A,j} \omega_j \right| \delta_{B,j}}{\sum_{j=1,I} \left| \nu_{A,j} \omega_j \right|} \times I_A \tag{50}$$

The importance index I is unity for all species on the importance list, and it will only reach unity for species B when it is the only species directly connected to another important species. After the evaluation of the index for B, if its value is greater than the threshold, the species is then added to the reduced mechanism and another iteration is made. This process continues till no further species can be added to the final mechanism.

In the DRG method, every time a species is added to the reduced mechanism its index becomes unity. DRGEP, on the other hand, will assume an index calculated by

$$I_B = \max\left[\max_{A \in \Omega}\left(\frac{\sum_{j=1,L} \left| \nu_{A,j} \omega_j \right| \delta_{B,j}}{\sum_{j=1,L} \left| \nu_{A,j} \omega_j \right|} \times I_A\right); I_B\right] \tag{51}$$

This causes the index of a species distant from the important ones to have a smaller value, thus resulting in a greater reduction of the mechanism in respect to DRG, even when assuming the same threshold value.

Figure 7 ilustrates an example of the application of DRGEP. The values listed close to the arrows represent the reaction rates. Following the example of Lebedev (2010), let species A be the important species and let the threshold for the important species be 0.3.

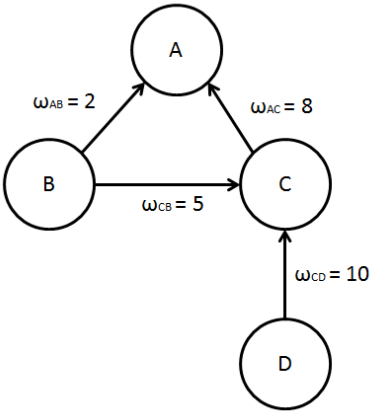

Figure 7 – Example of a Mechanism.
Adapted from Lebedev, 2010.

When applying the DRG method, one would obtain the following behavior:

Step 1 :

$$I_{AB} = \frac{\omega_{AB}}{\omega_{AB} + \omega_{AC}} = 0.2 < 0.3$$
$$I_{AC} = \frac{\omega_{AC}}{\omega_{AB} + \omega_{AC}} = 0.8 > 0.3$$

Conclusion: Add species *C* to the mechanism.

Step 2:

$$I_{CB} = \frac{\omega_{CB}}{\omega_{CB} + \omega_{CD}} = 0.33 > 0.3$$
$$I_{CD} = \frac{\omega_{CD}}{\omega_{CB} + \omega_{CD}} = 0.67 > 0.3$$

Conclusion: Add species *B* and *D* to the mechanism.

In this case, no reduction was achieved as no species could be removed. The DRG method does not take into account that species *B*

and *D* are not directly important for the initial species *A*, but instead they are important to *C*, and indirectly for *A*.

When using the DRGEP, the importance index for species *B* and *D* take the following values:

$$I_{AB} = I_{AC} \times I_{CB} = 0.8 \times 0.33 = 0.26 < 0.3$$
$$I_{AD} = I_{AC} \times I_{CD} = 0.8 \times 0.33 = 0.54 > 0.3$$

The conclusion is that only species *D* should be added to the mechanism, and the final reduced mechanism is then composed by species *A*, *C* and *D*.

Pepiot-Desjardins and Pitsch (2008), proposed the use of error propagation on DRG methods for systematic and fully automatic reduction of large kinetic mechanisms. They demonstrate the potential of DRGEP reducing an iso-octane kinetic mechanism composed by 850 species, obtaining, with the use of DRGEP, a 195 species, and after an additional QSSA, a 100 species reduced mechanism. Moreover, in the same study, they proposed an integrity check to avoid species on the reduced mechanism presenting only producing routes and no consumption paths, which may lead, in several cases, to large errors in simulations.

Shi et al. (2010) studied the use of automatic mechanism reduction using two-stage reduction, by first applying DRGEP and secondly a PCA to further reduce the mechanism. This approach was successfully applied to HCCI simulation to reduce the detailed mechanism of PRF fuels, n-heptane (561 species and 2539 reactions), iso-octane (857 species and 3606 reactions) and methyl decanoate (MD – 2878 species and 8555 reactions). The reduced mechanisms obtained present 140, 195 and 435 species respectively and were able to reproduce the detailed mechanisms over a set of conditions with about 25 % of the number of original species.

Bahouli et al. (2012) used a combination of DRGEP and CSP to generate a reduced n-heptane mechanism based on Curran's Mechanism (561 species and 2539 reactions). The DRGEP was used twice, before and after the application of CSP. The final mechanism (composed by 118 species and 330 reactions) achieved reduction rates of 79% for species and 87% for reactions, maintaining the error between the control parameter smaller than 2%. Furthermore, the final mechanism was able to reproduce the combustion phasing under HCCI conditions and mass fractions of O_2, CO and CO_2. The CPU time for calculating the cycle

using the reduced mechanism was 79 times smaller than the CPU time needed when using the full detailed mechanism.

Bahouli et al. (2014) performed a reduction on a combination of two kinetics mechanisms (GRI-Mech. 3.0, 53 species and 325 reactions, and Golovichev's mechanism, 57 species and 290 reactions, for natural gas and n-heptane fuels respectively). A single zone model for simulating the HCCI condition was used as data source for the reduction. A two-stage reduction scheme composed by first applying the DRGEP for removing unimportant species and then using a PCA method for removing redundant reactions was implemented. The reduced mechanism obtained present 19 species and 39 reactions for the GRI-Mech. 3.0 and 40 species and 95 reactions for the Golovichev's mechanism. A combined mechanism was then obtained for natural-gas/n-heptane and genetic algorithms were used to optimize the reaction rate constants. The final mechanism presents 109 reactions among 41 species and errors under 2º CA for the engine parameters used in the reduction.

2.5.3.4. Path Flux Analysis (PFA)

The Path Flux Analysis (PFA) follows the same approach of the DRGEP method, using the definition of error propagation through the kinetics mechanism to achieve a greater reduction. The main difference between PFA and DRGEP is how the importance index is evaluated. PFA uses the consumption and production flows to define it. Sun (2010) defines the consumption flow *C* and production flow *P* of a chemical species *A* as

$$C_A = \sum_{i=1,I} \max\left(-\upsilon_{A,i}\omega_i\,, 0\right) \tag{52}$$

$$P_A = \sum_{i=1,I} \max\left(\upsilon_{A,i}\omega_i\,, 0\right) \tag{53}$$

The flow rates between two species are defined as

$$C_{AB} = \sum_{i=1,I} \max\left(-\upsilon_{A,i}\omega_i\delta_B^i\,, 0\right) \tag{54}$$

$$P_{AB} = \sum_{i=1,I} \max\left(\upsilon_{A,i}\omega_i\delta_B^i, 0\right) \tag{55}$$

where δ_B^i was presented before on equation (47). The final contribution of species *B* to *A* for consumption and production are defined as

$$r_{AB}^{cons} = \frac{C_{AB}}{\max(P_A, C_A)} \tag{56}$$

$$r_{AB}^{prod} = \frac{P_{AB}}{\max(P_A, C_A)} \tag{57}$$

The importance index *I* is defined using the average of the two flows as

$$I_B = \max_{A\in\Omega}\left(\frac{r_{AB}^{prod} + r_{AB}^{cons}}{2} \times I_A\right) \tag{58}$$

The index I_A quantifies the indirect relation between species *A* and *B*. The application of this method follows the same sequence as the DRGEP.

Sun et al. (2010) used the PFA method in order to generate a reduced mechanism for n-decane and n-heptane, using different conditions for ignition, extinction and flame propagation. The reduced mechanism was tested against a DRG reduced mechanism and it was found that the mechanism generated using PFA could achieve a better accuracy than the larger DRG reduced mechanisms. Furthermore, Sun et al. demonstrated that the PFA reduced mechanism also worked well for unsteady combustion involving non-equilibrium flame structures and diffusive transport.

Li et al. (2013) performed a study in order to find out the redundant species and reactions based on the PFA method. They used it to reduce a detailed mechanism, proposed by Korobeinichebv et al. (2005) with 121 species and 682 reactions, for flame inhibited by phosphorus containing compounds. Using different thresholds, three reduced mechanism were obtained presenting 65, 60 and 55 species. The results for the reduced mechanisms for concentrations distributions of radical and major species agree with the results obtained from the detailed mechanism.

Gou et al (2012) developed and validated an approach of error controlled dynamic adaptive chemistry (EC-DAC) using PFA as a way to obtain local reduced mechanism. The method uses tabulated thresholds and the fuel oxidation progress variable as intake parameters. This leads to an error controlled kinetics model reduction which changes according to the local mixture, thus improving the computational time. Two kinetic mechanisms for homogeneous ignition of n-heptane/air and n-decane/air were used: a detailed one, composed by 1034 species and a reduced one with 121 species. The results showed that the EC-DAC can improve computational efficiency by more than one-order of magnitude for both mechanisms, being a great candidate to be used in direct numerical simulation of reactive flows.

2.5.4. Other Methods

There are several other strategies to reduce kinetics mechanisms, which are not described here, such as the Dijkstra algorithm to find the reaction path or genetic algorithms (GA) to obtain the best species list. These techniques either applied alone, or combined provide strategies to address specific problems.

The methods described here showed to be very effective in the reduction of chemical mechanisms for the combustion of hydrocarbons and will be applied in this work as described in the next chapter.

3. METHODOLOGY

3.1. Detailed Kinetics Mechanisms and Targets

For this study, three detailed chemical kinetics mechanisms for the ethanol combustion with air were chosen. They were those by Leplat (2011), Cancino (2010), and Mittal (2014). Table 4 presents a summary of the characteristics of each one. This choice was based on the generality and applicabitlity of the mechanisms. Leplat´s mechanism is a relatively small mechanism widely tested against species concentrations in PSR. Cancino was developed and tested for high pressure IDT measured in shock tube. Finally, Mittal´s is the most recently developed mechanism widely tested against shock tube and rapid compression machine IDT, laminar flame and PSR data.

Table 4 - Detailed chemical kinetics mechanisms for the combustion of ethanol and air.

Author	**Number of species**	**Number of reactions**	**NO_x chemistry**	**Transport data**
Leplat (2011)	38	252	No	Yes
Cancino (2010)	135	1349	Yes	No
Mittal (2014)	111	710	No	Yes

For the reduction of Leplat´s model, the laminar flame speed for a free premixed flame (FF) was used as target. For Cancino´s and Mittal´s models, a constant pressure, constant mass reactor model was used and the ignition delay time (IDT) was the target parameter.

3.2. Application of the reduction methods

Since the size of Leplat´s mechanism is smaller, in comparison to Mittal´s and Cancino´s, it was used to comparatively evaluate the methods, namely, the DSA, ROP, DRG, DRGEP, and PFA, and discuss several points of the methodology used. From this initial analysis, two methods, the DRG and DRGEP, were selected and applied to Cancino´s

and Mittal´s mechanisms. Since these are more complete mechanisms, they were used to evaluate the performance of the DRG and DRGEP methods and the challenges of their implementation. The performance parameters considered were efficiency, CPU time and ease of implementation. Figure 8 presents a diagram of the application of the reduction methods.

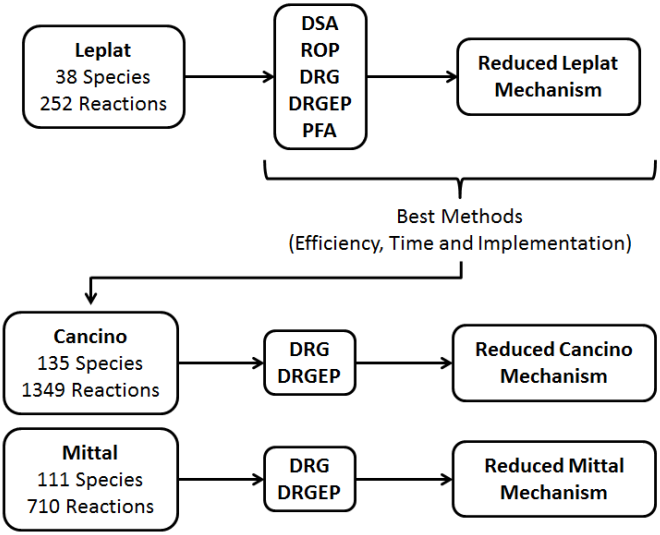

Figure 8 – Flowchart of the reduction sequence

The efficiency of each method was defined as the rate of species and reactions removed, in the average, at each iteration and were evaluated using

$$SRR = \frac{total\ number\ of\ species\ removed}{total\ number\ of\ iterations} \tag{59}$$

$$RRR = \frac{total\ number\ of\ reactions\ removed}{total\ number\ of\ iterations} \tag{60}$$

where *SRR* and *RRR* denote Species Removal Rate and Reactions Removal Rate, respectively. Methods with higher values of SRR and RRR are considered efficient.

The selection of the final reduced mechanism is based on the number of species, that is, the final mechanism for each detailed kinetics mechanism is the one with the smaller number of species.

3.3. Conditions for Reduction

The reduction conditions are defined as those for which the mechanisms are applied and their reduction is achieved. The Evaluation Conditions are those where both the detailed and the reduced mechanisms are tested and compared. Table 5 shows the conditions used for the reduction and for the evaluation of the reduction.

Only one temperature was used for the reduction, since the behavior for the other temperature is similar. However, two temperatures were used for evaluation. Only one pressure was used on the reduction and evaluation, but the final mechanism will be compared at 30 bar as well.

Table 5 – Conditions used for the reducing Leplat´s mechanism.

Reduction Conditions		
Equivalence ratio	**Temperature (K)**	**Pressure (bar)**
0.6	343	1
1.1	343	1
1.4	343	1
Evaluation Conditions		
Equivalence ratio	**Temperature (K)**	**Pressure (bar)**
0.6 to 1.4	343	1
0.6 to 1.4	298	1

The following reduction methods were used: DSA, ROP, DRG, DRGEP and PFA. As stated before, the Leplat's mechanism has the smallest number of species and reactions among the three chosen mechanisms, hence it was first used to evaluate the reduction methods and, then, to select the most promising approaches for the larger mechanisms.

The conditions used for reducing Cancino's and Mittal's detailed mechanisms are presented in Table 6. The methods selected for reduction in this case were the DRG and DRGEP.

Table 6 – Conditions used for reducing the Cancino's Mechanism and the Mittal's Mechanism

Reduction Conditions		
Equivalency ratio	**Temperature (K)**	**Pressure (bar)**
1	900	10
1	1200	10
1	800	30
1	1200	30
1	800	50
1	1200	50
Evaluation Conditions		
Equivalency ratio	**Temperature (K)**	**Pressure (bar)**
1	900 to 1200	10
1	800 to 1200	30
1	800 to 1200	50

For the species based reduction methods (DRG, DRGEP and PFA), the set of important species Ω selected for all the cases was composed by the fuel (C_2H_5OH), oxidant (standard air – O_2, N_2 and Ar), complete combustion products (CO_2, H_2O), carbon monoxide (CO) and the hydroxyl radical (OH). The formation of this set was based on the criteria that it should contain all the species that must be accurately described by the reduced mechanism. Here, only these were considered, but other applications could use a larger set, for example, including NOx species.

3.4. Algorithms for Application of the Reduction Methods

Due to the differences among the reduction strategies, different algorithms were implemented for the reaction based (DSA and ROP) and for the species based methods (DRG, DRGEP and PFA).

3.4.1. Reaction based methods (DSA and ROP)

The main issue on employing the DSA method for reducing kinetics mechanism is to determine how the sensitivity will be used. Taking as an example a constant pressure, constant mass reactor, at each transient point, for each species and temperature, a sensitivity matrix is available. The main question is which of them (species and temperature) are important and must be used for the reduction. Another question is what point in space/time will be used, since the sensitivity of each reaction changes as the chemical reaction evolves.

Here, this difficulty will be circumvented by applying the DSA on a laminar flame problem. The freely propagating flame model has a flow rate sensitivity that does not depend on axial position along the flame and, therefore, was the model used to test the DSA method. The application of the DSA method to a kinetics mechanism that does not have the complete set of transport data available, such as Cancino´s mechanism, becomes more complex and will not be discussed here as questions such as which sensitivities and how it will be used must be answered.

For the ROP method, a table similar to Table 3 was built and the important species list was used. Only the reactions for these species that have an index above a threshold were kept in the mechanism. The species represented on the final selection of reaction were added to the mechanism.

3.4.2. Species based methods (DRG, DRGEP and PFA)

The species based methods (DRG, DRGEP and PFA) work under basically the same algorithm. The difference between the three methods is how the importance index of each species is evaluated. This evaluation was reviewed on chapter 2. Figure 9 presents the general algorithm used for these methods.

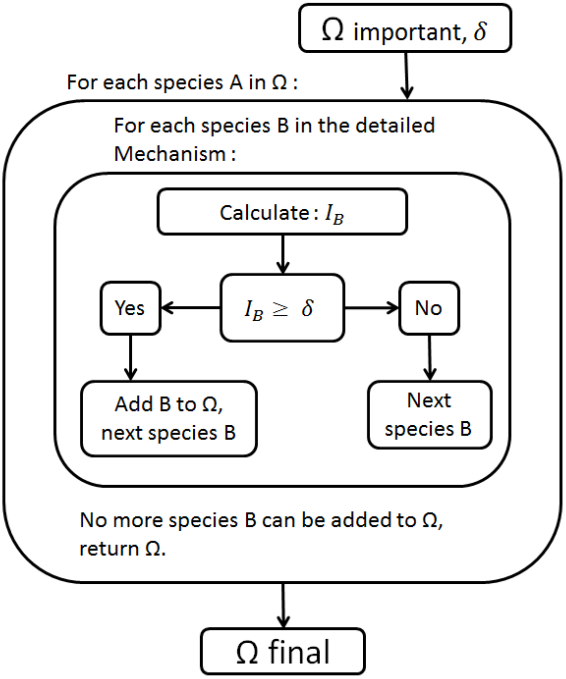

Figure 9 - Flowchart of reduction methods based on species.

The algorithm is explained as follows. Initially, the problem were the reduction is going to be applied is identified, and, for this problem, all points in time and space where the reduction will be attempted are chosen. This defines the domain (of points) were the reduction is performed and evaluated. The full detailed mechanism is used to solve the combustion problem generating the rate of reaction and rates of consumption and production of each species over (each point in) the domain. Starting on the initial point, the initial entries for the reduction are the important species list (Ω), which contains all the species that must be accurately described, the user defined threshold (δ), the matrix of stoichiometric coefficients, and the reaction rate data calculated for the given point in time and space under consideration. The importance index for all species in respect to a species A present in Ω is then calculated using equations (43), (51), or (58). Only those species whose importance index is greater than the threshold δ are added to Ω. This process continues for all species on Ω until, either no additional

species can be added, resulting in a reduced species list, or all species are added to the mechanism, returning in a failed reduction attempt.

Regarding how the different points on the domain are treated, the DRG method can follows two different strategies: A sequential and a parallel one.

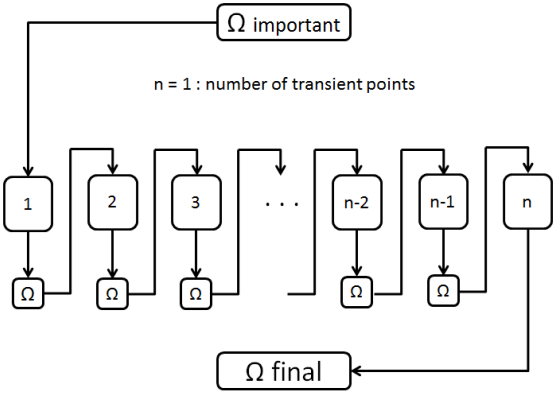

Figure 10 – Sequential reduction method.

On the Sequential approach, presented in Figure 10, the reduced mechanism obtained in a domain point *n* is used as the important species list (Ω) for the point *n*+1. As a consequence, on each new point, the reduction mechanism is at least equal or larger than the mechanism obtained in the previous point.

This approach tends to be much slower than the approach shown on Figure 11, generating a more conservative reduced mechanism with the same threshold limit.

On the Parallel strategy, presented on Figure 11, at each reduction point the algorithm starts from the same set of original species and may end up with a different set of species in each reduction point. Since in each point a small mechanism is obtained just for the local conditions, this approach is completed in a smaller computational time.

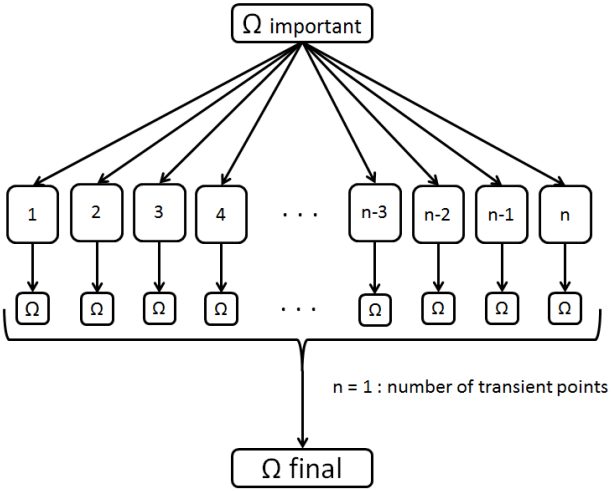

Figure 11 – Parallel reduction method.

This strategy is similar to the dynamic reduction methods generally employed in on-the-fly reductions. For a static reduction using this strategy, all the mechanisms obtained from all the domains points used for the analysis are united, generating a single static kinetics mechanism, which is, by definition, able to reproduce the detailed mechanism results in all of the conditions used.

As an example, using six different conditions of temperature and/or pressure, and using Cancino's mechanism with a 0.1 threshold, two reduced mechanism were obtained, one using a parallel DRG approach and the other using a sequential DRG. Figure 12 presents the evolution of both reduced mechanisms along the transient domain within the ignition delay period. The y-axis is the number of species in the reduced mechanism expressed as a percentage of the number of species in the detailed mechanism. The x-axis represents the simulation points, varying from the beginning of simulation up to 2 seconds. The time step between points is not constant, but chosen according to the time variation of the concentration of the chemical species. Therefore, there is a smaller time step near ignition. At each condition, the vertical steps in the curves represent the addition of one or more species to the final mechanism.

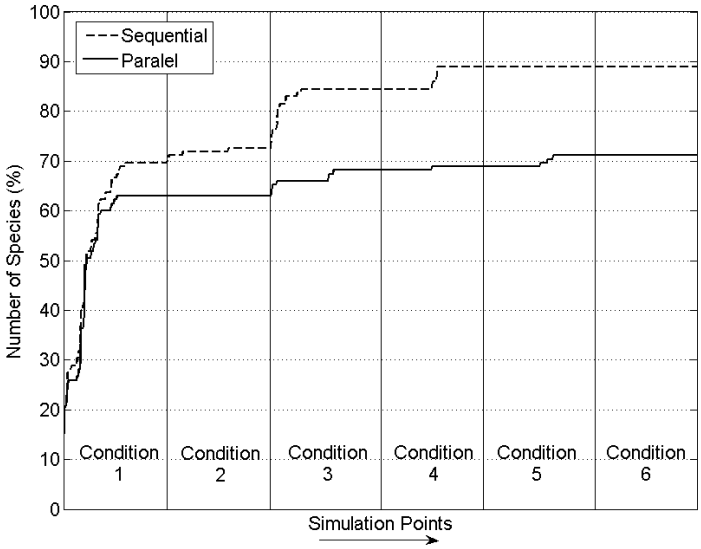

Figure 12 – Comparison of the mechanism size evolution of DRG parallel and DRG sequential with a threshold of 0.1.

The sequential reduced mechanism obtained has approximately 90% of the detailed mechanism species, whereas the parallel has a little more than 70%. It also possible to notice that, after a fast increase in the size of the mechanism, the number of species varies much slower for the remaining conditions. The CPU time spent running every condition on the sequential method was, at least, 30% higher than for the parallel.

Due to the fact that the DRGEP and PFA methods require an update of the index for each species every time a new one is added to the important list, both methods can only be used in the parallel strategy.

The algorithms were implemented in MATLAB® Release 2012a. The combustion problems were solved using ChemKin PRO.

4. RESULTS AND ANALYSIS

This chapter presents the reduced mechanisms obtained from the detailed mechanisms by Leplat (2011), Cancino (2010) and Mittal (2014). The analysis will consider the relative performance of the different reduction methods and the differences that arise in the reduced mechanisms. The comparison of the predictions of the detailed mechanisms for different combustion problems were explored lengthily in Demetrio (2010). For completeness, only an overview of the results of the problems solved is given below.

4.1. Solutions of the base problems

Leplat´s mechanim will be used to explore the solution of the base problems for a few conditions.The aim of this section is to present the physical results expected for each problem.

The basic evolution of the reaction paths in the ethanol combustion have been well explored (Cancino et al., 2010; Tran et al., 2013; Herrmann et al., 2014). Firstly, initiation reactions build the pool of radical species, especially H and O. In the following, ethanol (C_2H_5OH) undergoes pyrolysis and the attack of the radical species begining at 500 K. Following hydrogen abstraction, three radicals, CH_3-CH-OH, CH_2-CH_2-OH and CH_3-CH_2-O, are formed, depending on which H atom is removed from the ethanol molecule. The prediction of the branching ratios is very important for the mechanism. Hydroperoxy radical (HO_2) and methyl hydroperoxide (CH_3OOH) are formed primarily in the 500 - 800 K range. Hydrogen follows down to an H_2-O_2 submechanism. The H_2-O_2 submechanism is the main responsible for the propagation and ramification reactions following hydrogen peroxide (H_2O_2), hydroperoxy radical (HO_2), and the hydroxil radical (OH). Water (H_2O) is finally formed. Above 800 K, the radical (CH_3CHOH) decomposes forming acetaldehyde (CH_3CHO), acetyl radical (CH_3CO) and methyl radical (CH_3). This species follows to C1 mechanisms forming formaldehyde (CH_2O) and methane (CH_4). Radical CH_2CH_2OH follows to a C2 mechanism from ethylene (C_2H_4), to ethane (C_2H_6) and vinyl radical (C_2H_3), and to acetylene (C_2H_2). The carbon species finally form CO and CO_2. The configurations in the following sections evidence these reaction paths.

4.1.1. Laminar free premixed flame

A free premixed flame with initial temperature 343 K, pressure 1 bar and equivalence ratio Φ = 1 is chosen to present the basic results expected from the reduced mechanism. With the use of Leplat´s mechanism, the laminar flame speed obtained is 54 cm/s. This compares quite well with the value of 52.5 cm/s from measurements from Konnov et al. (2011). Figure 13 presents the distribution of temperature, molar fractions of C_2H_5OH, O_2, CO, CO_2, H_2 and H_2O. The profiles are scaled up to their maximum values in order to fit in the same graphic. Figure 15 presents the distribution of the molar fractions of HO_2, OH, H_2O_2, CH_4, CH_3, CH_2O, HCO, C_2H_6 and C_2H_2.

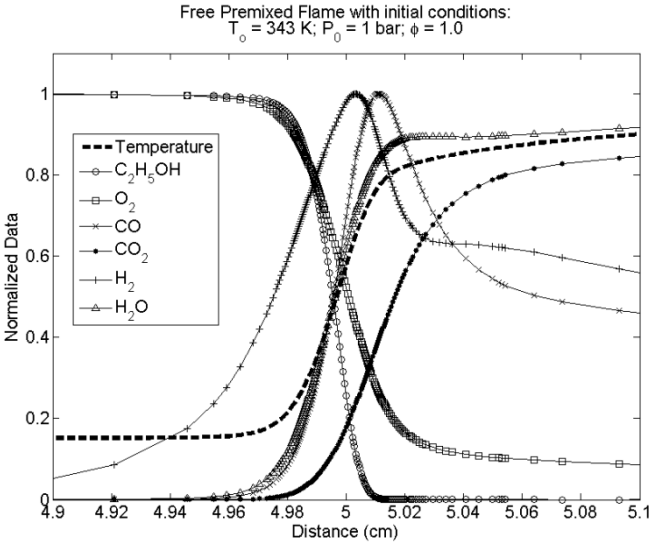

Figure 13 – Temperature and species molar fraction for a freely propagating premixed flame with initial conditions of 343 K, 1 bar of pressure and Φ = 1 using the Leplat's detailed mechanism.

Within the flame, two regions can be highlighted: the preheating zone and the reaction zone. Figure 14 (Turns, 2013) represents schematically these two regions. The first region is characterized by a balance between heat conduction and convection upstream from the flame. The second region presents two sub-regions, one characterized by fast chemical reactions, which are very thin, and a

wider sub-region, where most slow chemical reactions occur. The destruction of fuel and formation of several intermediates happens in the fast sub-region, presenting large temperature and concentration gradients. The second sub-region is mainly controlled by slow chemical reactions and can extend for several millimeters (Turns, 2013).

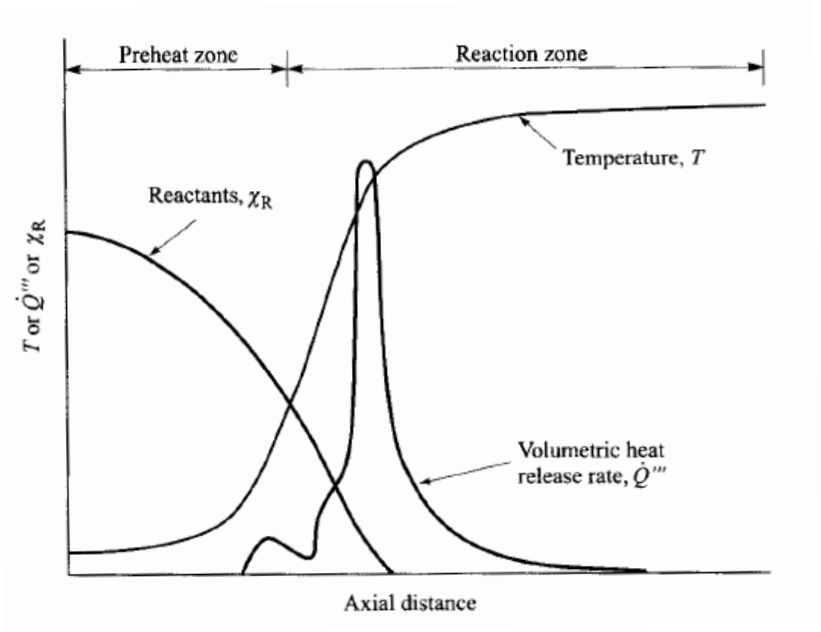

Figure 14 – Laminar flame structure.
Source: Turns, 2013

Figure 15 present several species concentration profile (normalized by their maximum). Ethanol is decomposed upstream in the flame. The intermediate species peak up progressively in the order H_2O_2, HO_2, CH_2O, C_2H_6, CH_4, C_2H_2, CH_3, HCO, and OH.

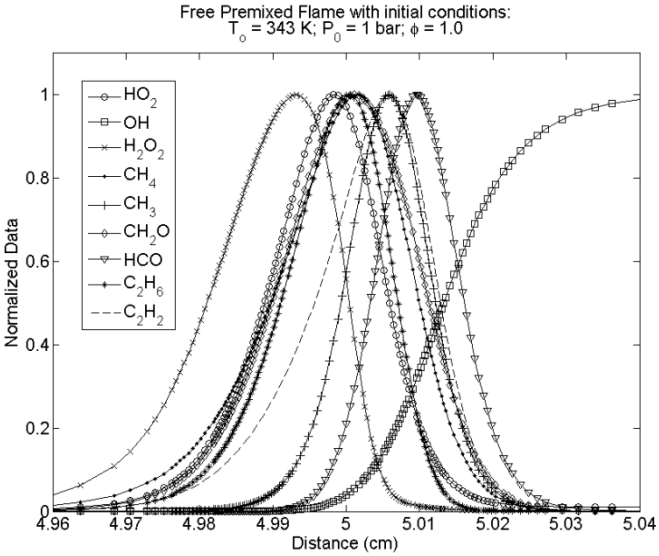

Figure 15 – Normalized species molar fraction for a free premixed flame with initial conditions of 343 K, 1 bar of pressure and Φ = 1 using the Leplat's detailed mechanism.

4.1.2. Ignition delay time in constant pressure, constant mass reactor

The thermal ignition at constant pressure, constant mass reactor is simulated using Leplat´s mechanism for initial temperature 1200 K, pressure 10 bar and equivalence ratio Φ = 1. Figure 16 presents the time evolution of temperature, molar fractions of ethanol, oxygen, carbon monoxide, carbon dioxide, hydrogen and water. The profiles are scaled up to their maximum values in order to fit in the same graphic. Figure 17 presents the time evolution of the molar fractions of HO_2, OH, H_2O_2, CH_4, CH_3, CH_2O, and HCO.

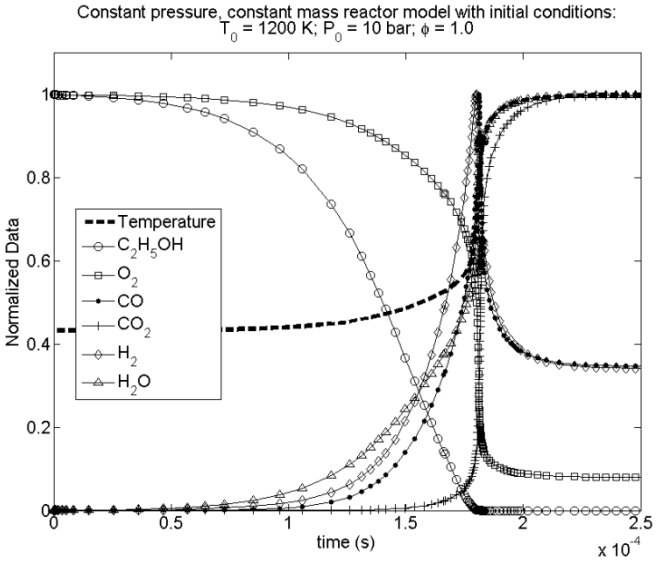

Figure 16 – Normalized temperature and species molar fractions for a constant pressure, constant mass reactor model with initial conditions of 1200 K, pressure of 10 bar and Φ = 1 using Leplat's detailed mechanism.

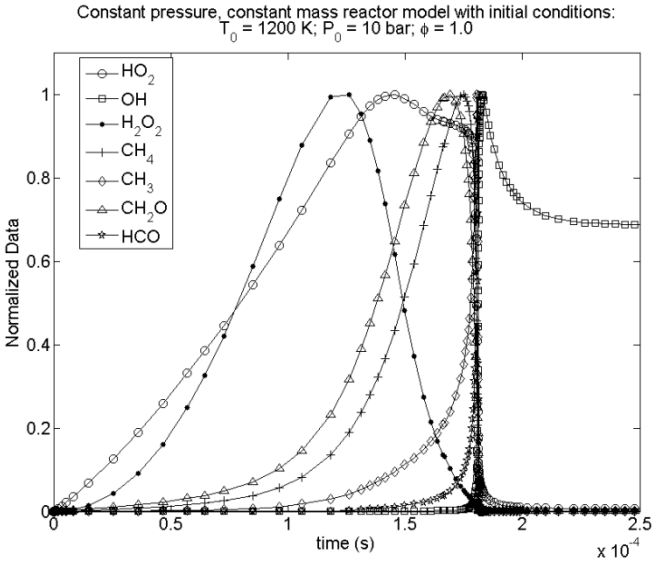

Figure 17 - Normalized species molar fractions for a constant pressure, constant mass reactor model with initial conditions of 1200 K, pressure of 10 bar and Φ=1 using Leplat's detailed mechanism.

The IDT time is defined here as the time it takes for OH to reach its peak concentration. This convention was used as it was the same employed by the authors to obtain the IDT values. The fuel is consumed earlier and several reactive intermediates are created, as evidenced in Figure 17. The intermediates presented peak up in the order H_2O_2, HO_2, CH_2O, CH_4, CH_3, HCO, and OH. This order closely reflects the reaction paths described above.

Results for other conditions and experiments are presented by Demetrio (2010).

4.2. DRG Algorithm Validation

For the validation of the DRG algorithm, the same mechanism for the ethylene oxidation (70 species and 463 elementary reactions, Qin et al., 2000) used by Lu and Law (2005) was reduced.

The final mechanism obtained here presents some differences in the final species set. The reduced mechanism obtained using a threshold of 0.16 and the DRG method by Lu and Law was composed by the following species: H_2, H, O, O_2, OH, H_2O, HO_2, H_2O_2, C, CH, CH_2, CH_2*, CH_3, CH_4, CO, CO_2, HCO, CH_2O, CH_2OH, CH_3O, CH_3OH, C_2H_2, C_2H_3,C_2H_4, C_2H_5, HCCO, CH_2CO, CH_2CHO, n-C_3H_7, C_3H_6, α-C_3H_5, Ar, and N_2. When using the same threshold, the final reduced mechanism obtained here presents all the species, excluding four, CH_3OH, n-C_3H_7, C_3H_6 and α -C_3H_5, and including C_2H as an additional species. These differences can be attributed to the fact that different points were used for the reduction, since the same results are only expected to be attained when using exactly the same points.

Figure 18 and Figure 19 present the size of the reduced mechanism of Lu and Law (2005) and the mechanism obtained here along the reduction process. We notice that the steps in the reduction are different by the same reason pointed out above. Overall, the agreement is considered adequate and the implementation is considered validated. The DRGEP and PFA methods were not validated since their code structure are the same of the DRG.

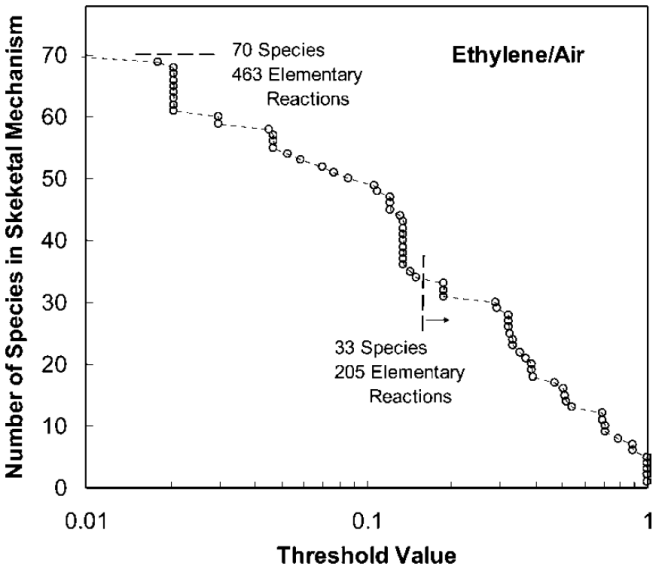

Figure 18 - Dependence of the species number of the skeletal mechanism on the threshold value.
Source: Lu and Law (2005)

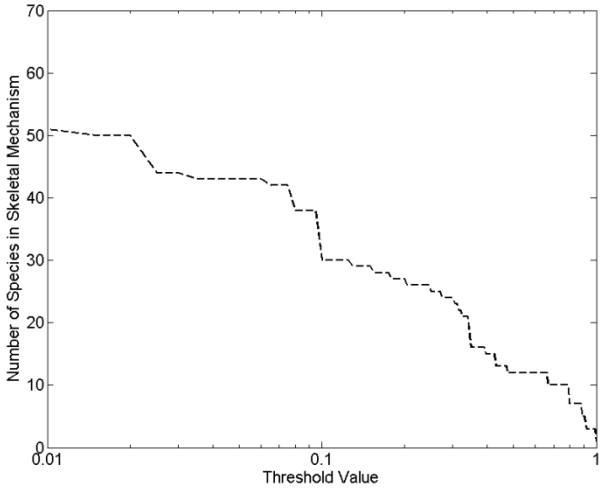

Figure 19 - Dependence of the species number of the skeletal mechanism on the threshold value using the implemented DRG algorithm.

4.3. Reduced Mechanisms from Leplat's Base Mechanism

As mentioned before, the reduction of Leplat´s model is developed in an exploratory way. In this analysis, the completed laminar flame speed is taken as the reduction target. Then, the predictions of the reduced mechanisms are compared to those of the detailed mechanism for the laminar flame speed (Figure 20, Figure 21, Figure 22 and Figure 23), the concentration of species along the flat flame (Figure 24 and Figure 25), the ignition delay time (Figure 26, Figure 27 and Figure 28) and the concentration of species along the ignition delay (Figure 29).

Table 7 presents the number of species and reactions obtained in the final reduced mechanisms generated using DSA, ROP, DRG, DRGEP and PFA. The number within parenthesis is the percentage in respect to the full detailed mechanism.

Table 7 – Number of species and reactions for each reduced mechanism

Mechanism	**Number of Species**	**Numberof Reactions**
Leplat (base)	38	252
DSA	35(92%)	133(53%)
ROP	38(100%)	189(75%)
DRG	33(87%)	180(71%)
DRGEP	32(84%)	182(72%)
PFA	37(92%)	227(90%)

The ROP and PFA methods presented the worst reduction in terms of number of species. The DRGEP method obtained the smaller mechanism in respect to the number of species, with 32 species, followed by the DRG with 33 species. Concerning the reactions, the DSA method achieved the larger reduction (with 53% of reactions from the detailed mechanism) followed by the DRG (with 71% of reactions).

The DSA method focus on finding the less important reactions to the target, therefore explaining the larger reduction of the number of reactions before reaching the maximum error or convergence issues. Being a reaction-focused method causes the reduction of the number of species to be a consequence of the smaller reaction set, thus providing reduced mechanisms with greater number of species. On the other hand, the DRG is devoted to finding the unimportant species, explaing why the smaller species mechanism were obtained via methods with the same concept (DRG and DRGEP). The removal of reactions is, therefore, a consequence of the presence of the species in the reduced

mechanism. The mechanisms obtained via species-based methods present larger reactions sets, since even the unimportant ones are included.

4.3.1. Reduction Targets Prediction

Figure 20 to Figure 25 present the results of laminar flame simulation using the detailed mechanism from Leplat and the reduced mechanisms obtained with the different methods.

Figure 20 and Figure 21 give the computed laminar flame speed as a function of equivalence ratio for a free flame with reactants at 343 K and 1 bar and equivalence ratio from 0.6 to 1.4. The initial threshold was set at 0.02 value. The maximum difference found between the reduced and detailed mechanisms over the simulated range of equivalence ratio is 5%, being larger for the rich flames. The best accuracies are found with PFA and DRGEP.

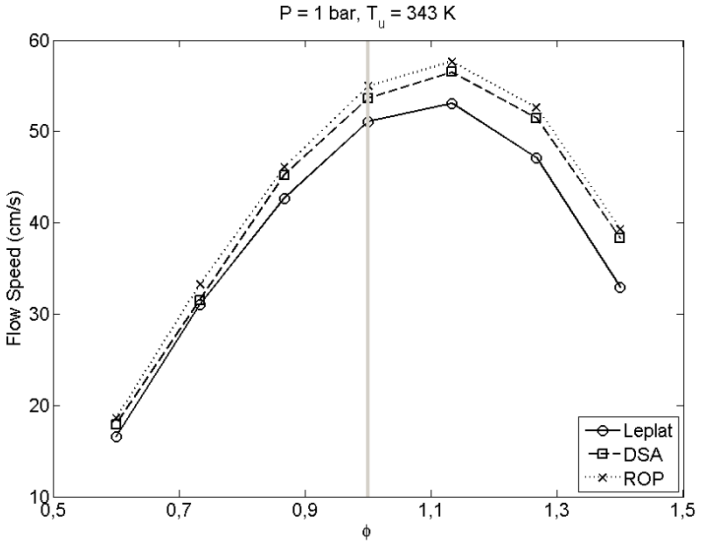

Figure 20 - Laminar flame speed for various mechanisms (Leplat's, DSA and ROP) at pressure of 1 bar and 343 K temperature.

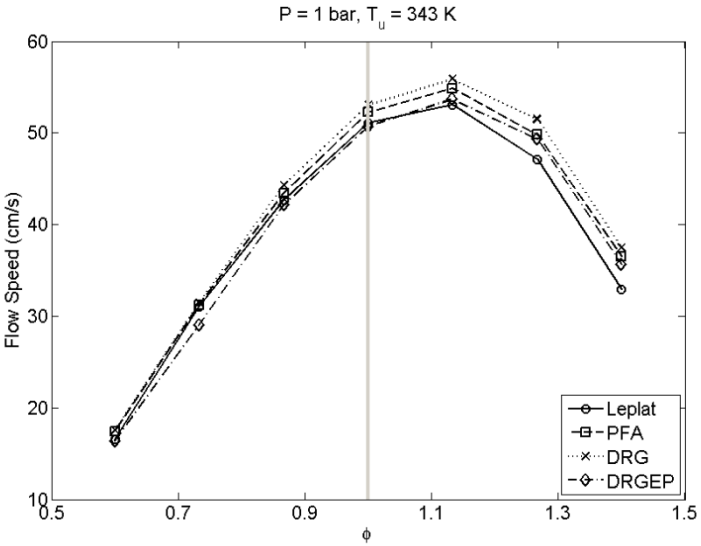

Figure 21 - Laminar flame speed for various mechanisms (Leplat's, PFA, DRG and DRGEP) at pressure of 1 bar and 343 K temperature.

Figure 22 and Figure 23 present the predictions for 30 bar. The maximum difference found between the reduced and detailed mechanisms over the simulated range of equivalence ratio is 25%. We recall that the reduced mechanisms have not been reduced for this condition of pressure. Insteac, they have been reduced at 1 bar and, then, applied at 30 bar. The uncertainty in predicting the laminar flame speed increased from 5%, in the pressure where the mechanism was reduced, to 25%. However, DSA and PFA resulted in accurate mechanisms.

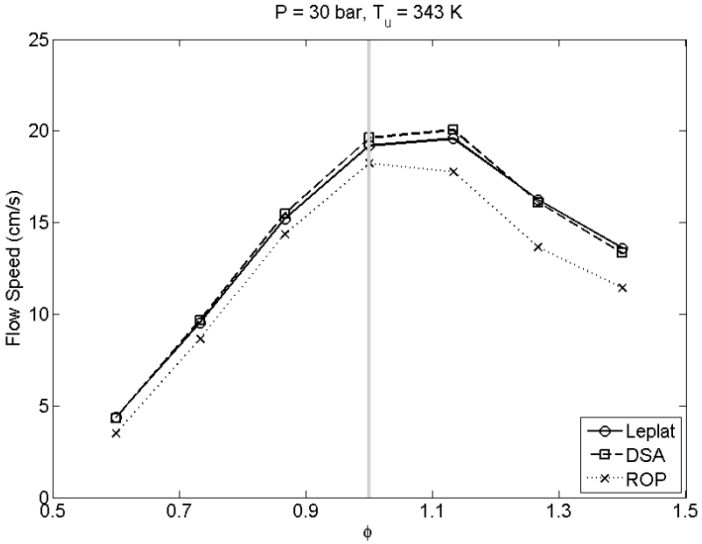

Figure 22 - Laminar flame speed for various mechanisms (Leplat's, DSA and ROP) at pressure of 30 bar and 343 K temperature.

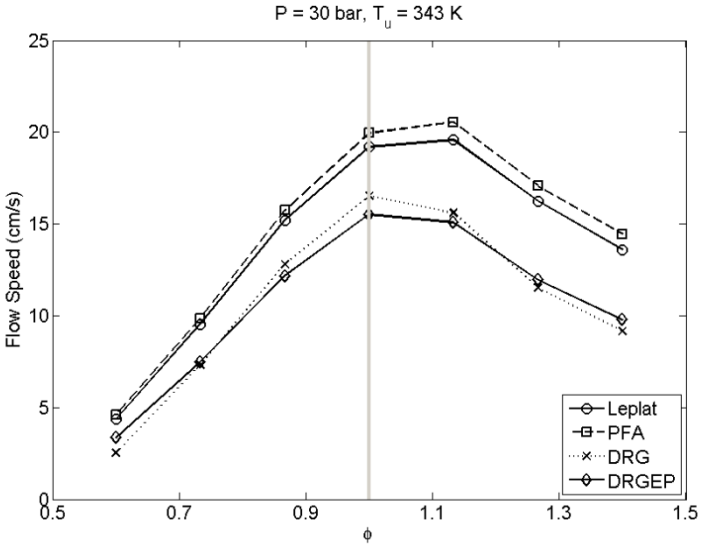

Figure 23 - Laminar flame speed for various mechanisms (Leplat's, PFA, DRG and DRGEP) at pressure of 30 bar and 343 K temperature.

The reduction obtained at 1 bar is analyzed further. Figure 24 and Figure 25 presents the axial mole fractions of the species considered important for the reduction (C_2H_5OH, O_2, CO_2, CO, OH, H_2O) for the equivalency ratio of 1.13 usign DSA and ROP methods. The difference is always smaller than 6%. The only noted difference is for OH predicted by the reduced mechanism obtained using ROP, which reaches a 5% discrepancy in the post flame zone. Figure 25 presents the results from the mechanisms reduced using PFA, DRG and DRGEP. The results present a difference everywhere smaller than 8%. The maximum deviations occur for CO and OH and are of 8% and 4% for the method DRGEP. This agreement is overall assumed to be very good. The results for the other reduction conditions present similar behavior and are not shown here.

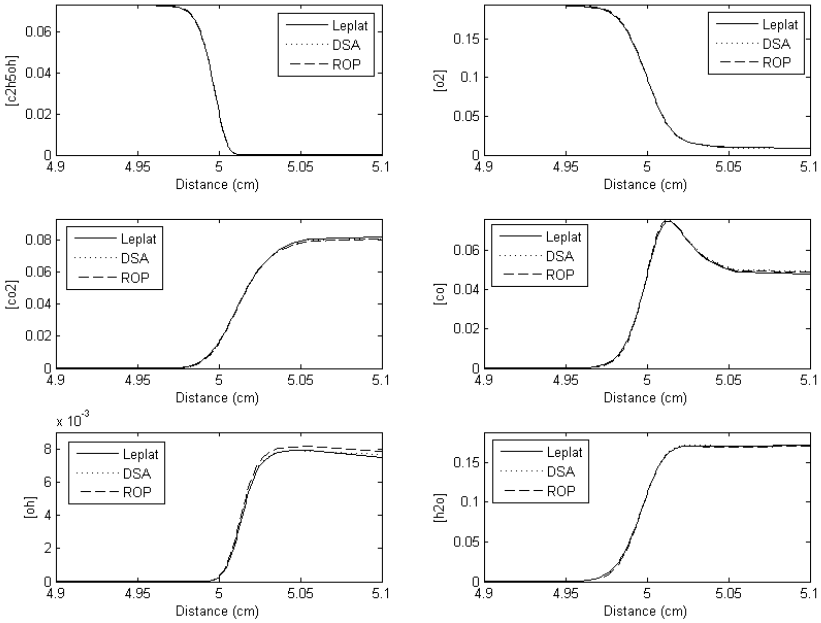

Figure 24 – Comparison between predictions using the reduced mechanisms (DSA and ROP) and the base mechanism for the important set of species.

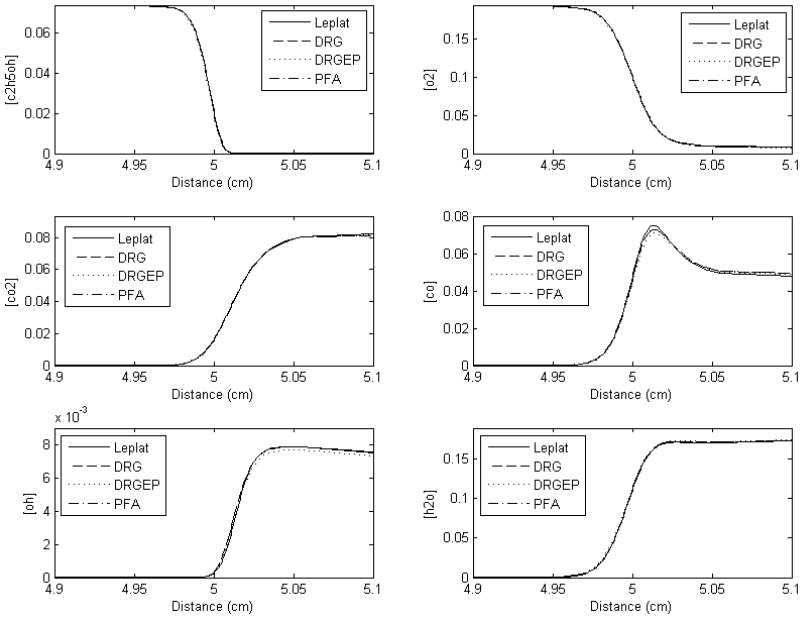

Figure 25 – Comparison between predictions using the reduced mechanisms (DRG, DRGEP and PFA) and the base mechanism for the important set of species.

Figure 26, Figure 27 and Figure 28 present the predictions of IDT using the reduced and detailed mechanisms. At 10 bar, the ROP reduced mechanism exhibits almost 3 times the IDT of the detailed mechanism at low temperature (900 K). The DSA, DRG and PFA presented better agreement, with a maximun deviation of 13.6% at 1200K using the DRG method. The DRGEP predicted the IDT with a maximum error of 49% at 1200K and 10 bar pressure, representing an absolute deviation in the order of 100 μs. The IDT deviation of the reduced mechanisms from the detailed mechanism decreases with the increase of pressure.

The relatively large errors are mainly associated to the fact that the reduction methodology employed here used the laminar flame speed problem to reduce Leplat's mechanism. Also, the larger threshold values, mainly for the ROP method, needed for the later iterations during reduction, resulted in worse predictions. Nevertheless, the DSA, DRG, PFA and, to certain extent, the DRGEP methods presented an acceptable accuracy.

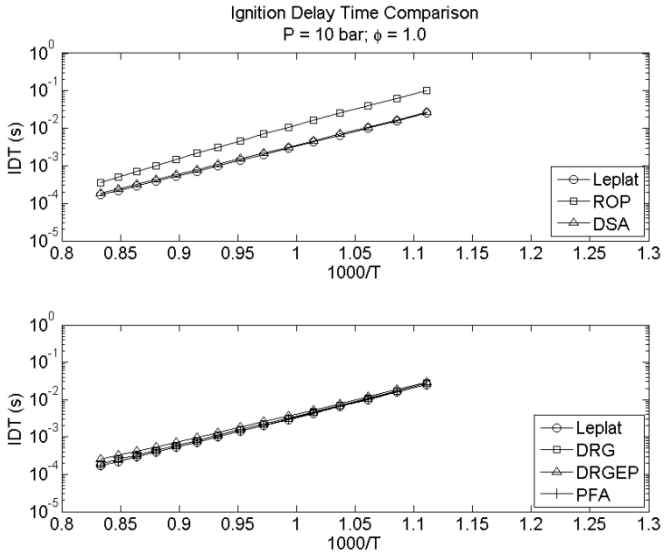

Figure 26 - Ignition Delay times comparison of detailed kinetics mechanism of Leplat with the reduced mechanisms. Stoichiometric mixture at 10 bar.

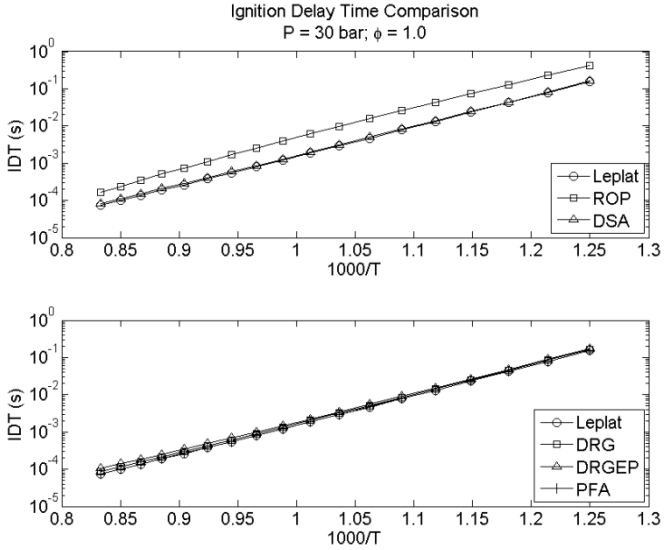

Figure 27 - Ignition Delay times comparison of detailed kinetics mechanism of Leplat with the reduced mechanisms. Stoichiometric mixture at 30 bar.

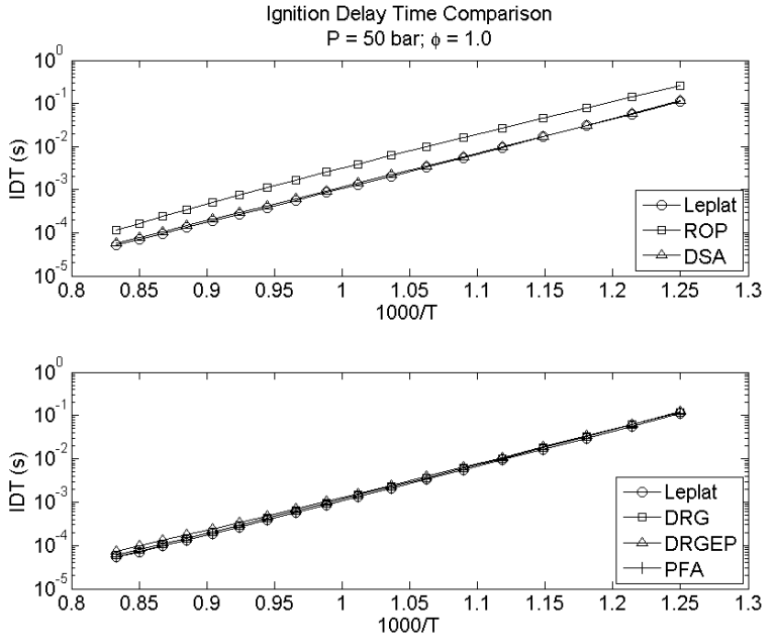

Figure 28 - Ignition Delay times comparison of detailed kinetics mechanism of Leplat with the reduced mechanisms. Stoichiometric mixture at 50 bar.

Figure 29 presents the evolution of the molar fraction for all methods used, except for ROP, for the IDT. All reduced mechanisms overpredict the IDT in respect to the detailed mechanism. The DSA and DRG methods presented almost identical molar fraction profiles, slightly phased from the solution using Leplat's mechanism. The PFA method presented a negligible difference whereas the DRGEP presented the largest deviation.

The selection of parameters to control the reduction, as well as the conditions in which the final reduced mechanism can be used are modeler´s choices and must be observed when generating reduced mechanisms, since they impact the accuracy and applicability of the final reduced mechanisms.

In the following, the rate of reduction is analyzed in order to determine the computational advantage of each method.

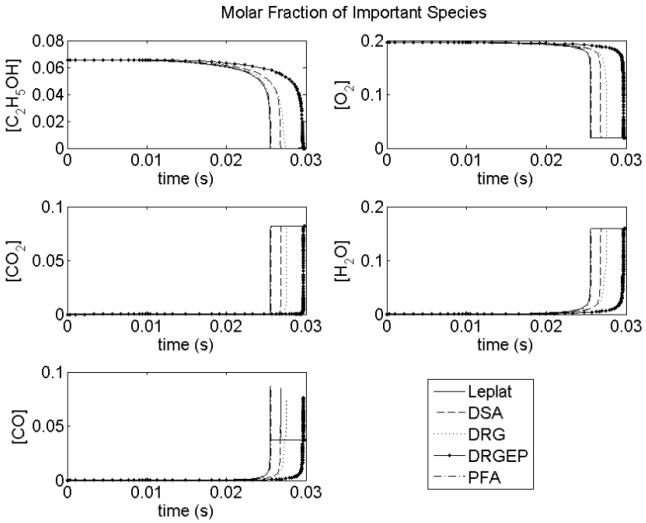

Figure 29 - Comparison of molar fraction of the important species for the IDT model at 10 bar of pressure and Temperature of 900K.

4.3.2. Rate of Reduction of the Different Reduction Methods

An important outcome when employing reduction methods is the time spent to reduce the detailed mechanism. The methods based on species removal should present a faster reduction rate than the methods based on reactions. Table 8 presents the number of iterations needed to obtain the reduced mechanism, the species rate of removal, which is the number of species removed divided by the number of iterations, and the reactions rate of removal, defined as the number of reactions removed divided by the number of iterations.

Table 8 – Comparison of the efficiency of the reduction methods for the reduction of Leplat's detailed mechanism.

Method	**Iterations**	**Species Removal Rate[1] (SRR)**	**Reaction Removal Rate[2] (RRR)**
DSA	32	<1	3,7
ROP	8	0	7,9
DRG	3	1	24,0
DRGEP	3	2	23,3
PFA	2	<1	12,5

[1] Number of total species removed divided by the number of iterations;
[2] Number of total reactions removed divided by the number of iterations.

The higher number of iterations needed in the DSA approach and the low reduction rates achieved evidences the difficulty of using the DSA method for very large mechanisms with several reduction conditions.

The methods devoted to removing species presented a small number of iterations allied with higher reduction rates. Although the PFA is a species-based method, the reduction is very poor, when compared to the DRG and DRGEP. Therefore, the good prediction of IDT obtained with the PFA method is a result of the smaller reduction achieved and, therefore, is not desired as a reduction method. The DRG and DRGEP methods ought to, then, be preferred due to the larger rates of reduction.

Finally, it is important to note that even though the mechanisms obtained via DRG and DRGEP are characterized by almost the same number of species and reactions, the final mechanisms were different as the species remaining were not the same.

4.3.3. Threshold Choice Effect

The DRG method has been used to evaluate the effect of the choice of threshold on the size of the reduced mechanism. Figure 30 presents the size of the reduced mechanisms found at each position along the freely propagating premixed flame, with unburned conditions of 343 K and 1 bar, for two levels of threshold, 0.01 and 0.1, and three equivalence ratios. The threshold of 0.01 is a 1 % cut-off, meaning that only species with consumption/production influence on the important species with lager values are kept on the mechanism. The flame is anchored at position x = 5 cm. The mechanism required to capture the initial part of the preheating zone is relatively smaller. As the temperature rises and more intermediate species are produced, the mechanism size needed grows. Near the equilibrium zone, where only the termination reactions prevail, the mechanism size needed is reduced again. The full (original) mechanism is needed for the 1 % threshold in most of the reaction zone. A reduction in 8 species is possible when the acceptable threshold is relaxed to 10 %. This may be a significant reduction when dealing with a problem where there is no need for a higher accuracy.

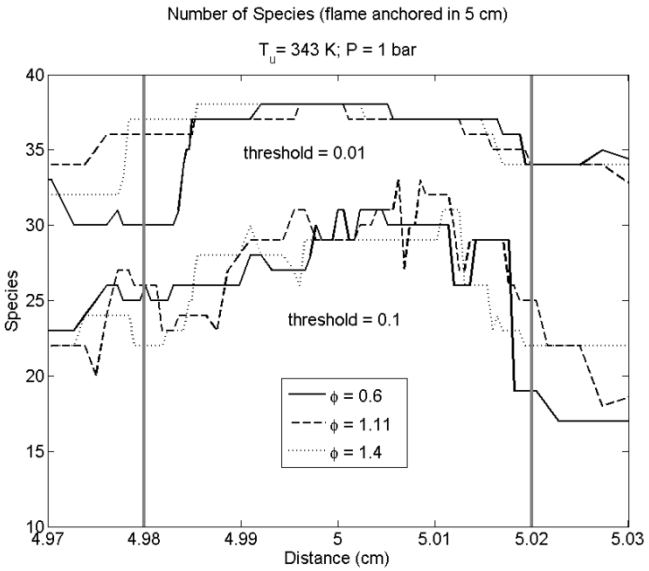

Figure 30 – Size of the reduced mechanisms obtained at each axial position along a freely propagating constant pressure laminar flame, with unburned conditions of 343 K and 1 bar, from Leplat´s detailed mechanism using the DRG method.

Figure 31 presents the size of the reduced mechanisms found at each position along the freely propagating premixed flame, with unburned conditions of 343 K and 30 bar, for two levels of threshold, 0.01 and 0.1, and three equivalence ratios. The flame is anchored at position x = 5 cm. At 30 bar and the threshold of 10 % we notice a further reduction in the end of the preheating zone, where the number of species in the reduced mechanism drops below 25. At the high pressure limit, the unimolecular decompositions become less dependent on temperature and peaks earlier (Cancino, 2009).

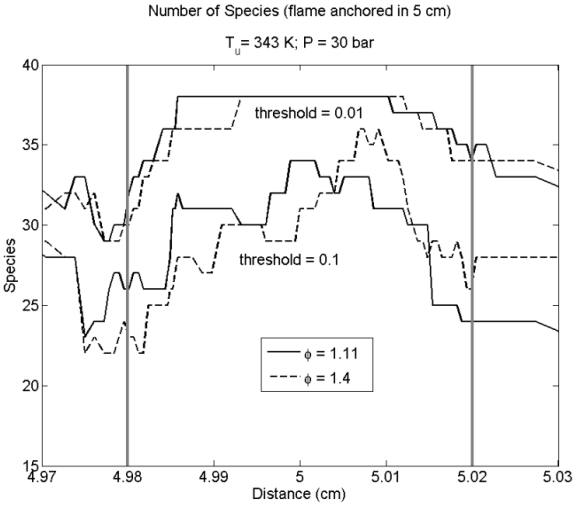

Figure 31 - Size of the reduced mechanisms obtained at each axial position along a freely propagating constant pressure laminar flame, with unburned conditions of 343 K and 30 bar, from Leplat´s detailed mechanism using the DRG method.

4.4. Reduced Mechanism from Cancino's Base Mechanism

Starting from the analysis of the reduction of Leplat's mechanism obtained results, the DRG and DRGEP have been chosen as the methods for reducing Cancino's mechanism. Also, the parallel and sequential approaches for DRG are evaluated here using the detailed mechanism proposed by Cancino.

Table 9 presents the summary of the reduced mechanisms obtained from the Cancino's detailed mechanism in terms of number of species and reactions.

Table 9 – Total number of species and reactions for the reduced mechanisms obtained from Cancino´s detailed mechanism.

Mechanism	Number of Species	Numberof Reactions
Cancino (Base)	135	1349
DRG – Sequential	125 (92%)	1291 (96%)
DRG – Parallel	92 (68%)	997 (74%)
DRGEP	79 (58%)	821 (61%)
DRGEP (excluding NOx chemistry)	45 (33%)	419 (45%)

As previously mentioned, 34 nitrogen related species on the full mechanism plus N_2 have been kept as the main focus is reduce the hydrocarbon oxidation mechanism.

The DRG – Sequential strategy stopped the reduction after few iterations due to convergence problems. The mechanism obtained from this method has almost no reduction, when compared against the others. For the DRG – Parallel strategy, the reduction stopped at 90 species due to convergence problems in one of six cases. The DRGEP method achieved an error larger than 7% with a reduced mechanism with 77 species. When excluding the nitrogen species, the DRGEP method results in a reduced mechanism with 45 species, representing 33.3% of the detailed mechanism, which represents an excellent compromise.

4.4.1. Reduction Targets Prediction

The reduction used the IDT as target. Thus, the comparison between the base and reduced mechanisms, shown in Figure 32, Figure 33 and Figure 34, presents excellent agreement. The maximum discrepancies between the predictions of all reduced mechanisms in respect to the detailed mechanism remains below 2 %. Although the maximum error tolerated for the reduction was fixed on 5 %, only the DRGEP stopped the reduction due to a larger IDT error.

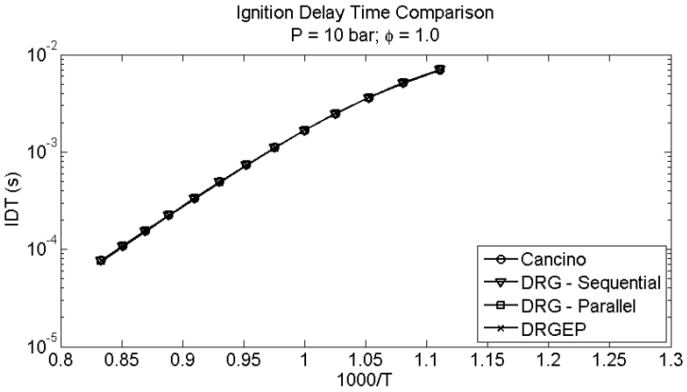

Figure 32 - Ignition Delay times comparison of detailed kinetics mechanism of Cancino with the reduced mechanisms obtained via DRG and DRGEP. Stoichiometric mixture at 10 bar.

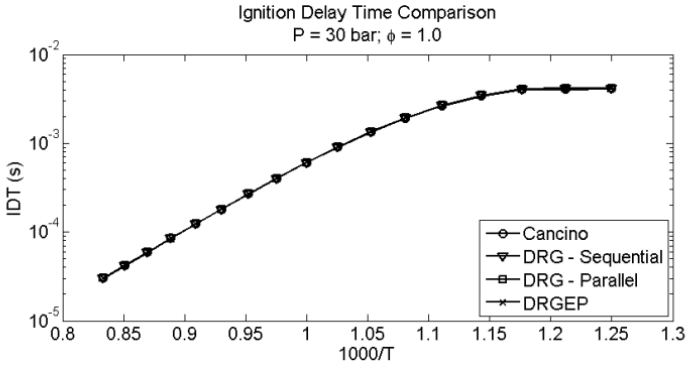

Figure 33 - Ignition Delay times comparison of detailed kinetics mechanism of Cancino with the reduced mechanisms obtained via DRG and DRGEP. Stoichiometric mixture at 30 bar.

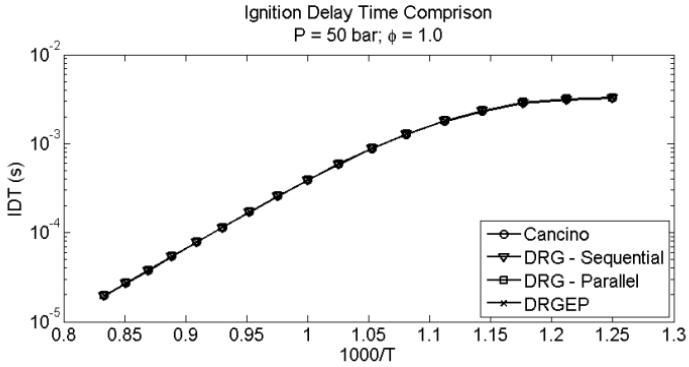

Figure 34 – Ignition Delay times comparison of detailed kinetics mechanism of Cancino with the reduced mechanisms obtained via DRG and DRGEP. Stoichiometric mixture at 50 bar.

Figure 35 shows the predictions comparison of the species molar fraction at the important list used for the reduction along the ignition delay, predicted using the reduced mechanisms and Cancino´s detailed mechanism for the stoichiometric mixture at 10 bar.

For all the species on the important, the comparison between the final reduced mechanisms with the detailed one show that the final mechanism can reproduce the results without a significant deviation.

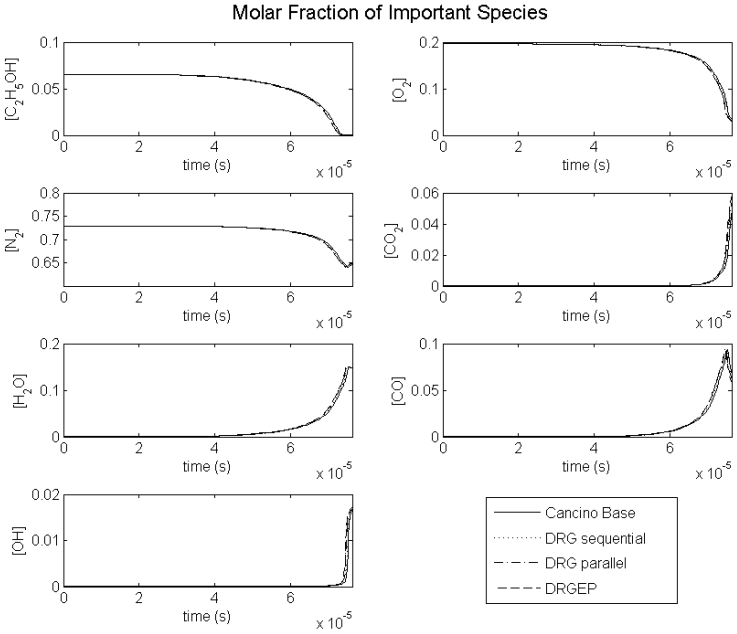

Figure 35 – Comparison of molar fraction of the important species for the IDT model at 10 bar of pressure and temperature of 900K.

4.4.1. Rate of Reduction of the Different Reduction Methods

Table 10 presents the number of iterations and the reduction rate for species and reactions.

Table 10 – Reduction rate of the reduction methods as applied to Cancino's detailed mechanism.

Method	**Iterations**	**Species Removal Rate[1] (SRR)**	**Reaction Removal Rate[2] (RRR)**
DRG – Sequential	3	3	19
DRG – Parallel	8	5	44
DRGEP	7	8	75

[1] Number of total species removed divided by the number of iterations;
[2] Number of total reactions removed divided by the number of iterations.

As expected, the DRGEP method achieves the faster reduction, with an average of 8 species per iteration which causes an average of 75 reactions removed at each step. The DRG – Sequential performed worse when compared to the DRG – Parallel method.

The evolution of the reduction process can be observed in Figure 36, where size of the reduced mechanisms, obtained with each method, is presented as a function of the threshold used.

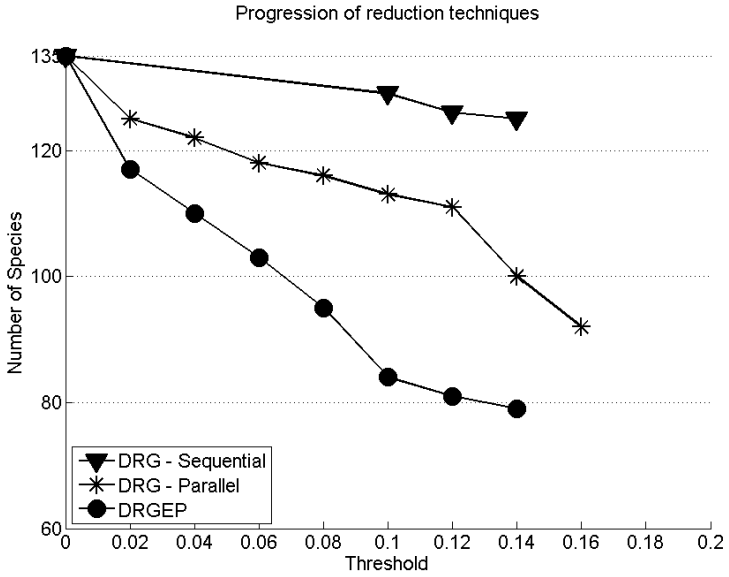

Figure 36 – Progression of different reduction techniques for the Cancino's detailed mechanism.

With the same threshold, the DRGEP method achieves a much greater reduction than the DRG methods, maintaining the error between the mechanisms at the same level.

In order to evaluate the static mechanism size, a one-step-reduction has been performed using the same final threshold for the DRG method and the size of each independent mechanism along the ignition delay is presented in Figure 37 for 900 K and 10 bar. The ignition delay time is identified by the vertical line.

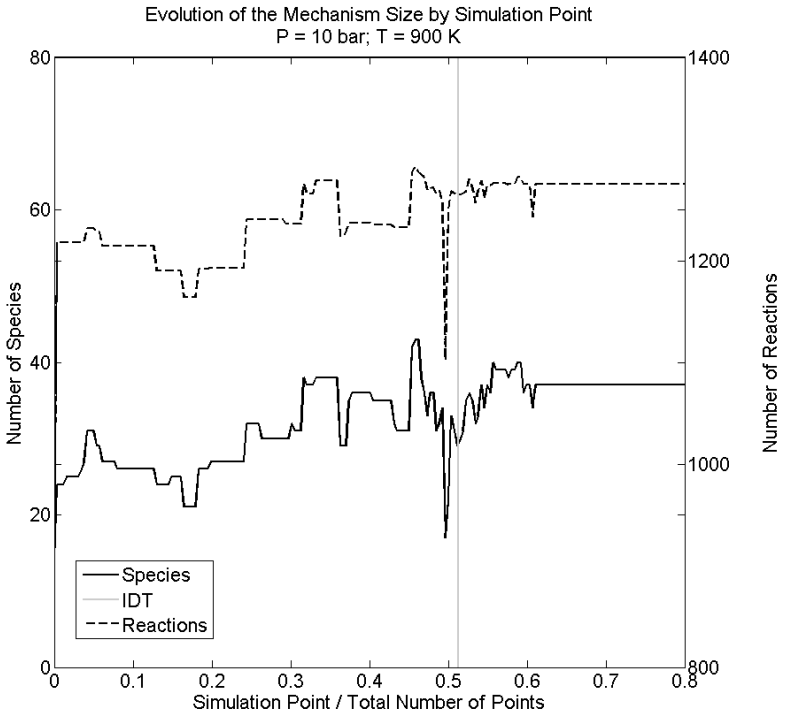

Figure 37 – Evolution of the size of the mechanism for a given condition and using an one-step DRG with a threshold of 0.16, for 900 K and 10 bar. The ignition delay time is identified by the vertical gray line.

This figure allows to verify that, in average, the size of the static mechanism grows as more intermediate species are created, achieving a maximum immediately before the IDT. The post IDT points present a large number of species, since the final reaction products are still in formation. The final mechanism obtained from the one-step DRG method, using the same threshold of the DRG – Parallel final step produces a much larger mechanism. Although only one set of initial condition is presented, the other conditions considered present similar results.

```
                Point/IDT Points - From 0.01 to 1.00, steps of acc. 0.04

O               x x x x x x x x - x x x x x x x x x x x x x x x x x x x x
H               - x x x x x x x x x x x x x x x x x x x x x x x x x x x x
H2              - x x x x x x x x x x x x x x x x x x x x x x x x x x x x
HO2             x x x x x x x x x x x x x x x x x x x x x x x x x x x x x
H2O2            - - x x x x x x x x x x x x x - - - - - - - - - - - - -
HCO             - x x x x x x x x x x x x x x x x x x x x x x x x x - x
CH4             - - - - - - - - - - - x x x x x x x x x x x - - - - - -
CH3             - x x x x x x x x x x x x x x x x x x x x x x x x - x
CH2O            - x x x x x x x x x x x x x x x x x x x x x x x x - x
CH3O            - - - x x x x x x x x x x x x - - - - - - - - - - - -
CH2             - x x x x x x x x - x x x x x x x x x x x x x x - x
CH              - - - - - - - - - - x x x x - - x x x - x x x x x x - -
SCH2            - x x x x x x x x - x x x x x x x x x x - - - x - x
C2H6            - x x x - - - - - - - - - - - - - - x x x x x x - - -
C2H5            x x x x - - - - - - - - - - - - - - x x x x x x x - x
CH3HCO          - x x x x x x x x x x x x x x x x x x x x x x x x - x
C2H4            x x x x x x x - - - - - - - - - - x x x x x x x x x x
CH2HCO          - - x x x x x x x x x x x x x x x x x x x x - - x - -
CH2CO           - - - x x - - - x x x x x x x x x x x x x - - x - -
C2H3            - - - - - - - - - - - - - - - - - x x x x x x x x x x
C2H2            - - - - - - - - - - - - - - - - - x x x x x x x x - x
HCCO            - - - - - - - - - - - - - - - - - x x x x x x x x - x
C2H             - - - - - - - - - - - - - - - - - x x - x x x x x - - -
CH3OH           - - - - - - - - - - - - - - - - - - - - - - - - - - - x
CH2OH           - - - - - - - - - - - - - - - - - - - - - - - - - x x - x
CH3CO           - x x x x x x x x x x x x x x x x x x x x x x - - x - -
C2H5O           - x x x x x x x x - - - - - - - x x x x x x x x x - x
SC2H5O          x x x x x x x x x x x x x x x x x x x x x x x x x - x
C3H4            - - - - - - - - - - - - - - - - - - - - - - - - - x - -
PC3H4           - - - - - - - - - - - - - - - - - x x - - - - - - x - -
C3H3            - - - - - - - - - - - - - - - - - x x - x x x x x x - -
IC4H3           - - - - - - - - - - - - - - - - - - - - x x x x x - - -
C4H2            - - - - - - - - - - - - - - - - - - - - x x x x x - - -
C3H2            - - - - - - - - - - - - - - - - - - - - x x x x x - - -
C6H6            - - - - - - - - - - - - - - - - - - - - - - - - - x x - -
PC2H5O          x x x x x x x - - - - - - - - - - x - - - - - - - - x x

                Legend:
                (x) is Present || (-) is Absent
```

Figure 38 – Presence of species on each simulation step till the ignition for one condition using an one-step DRG for Cancino´s mechanism for 900 K and 10 bar.

Figure 38 shows the presence of species (flagged as a "+" sign) at some simulations points before IDT when using the one-step method for 900 K and 10 bar. The last column represents the ignition point and the time step between each column is not constant, since the CHEMKIN utilizes a variable time step for improved solver accuracy and efficiency. The points on the right side are more closely spaced in time than the points on the left. Another observation is the fact, that not all time steps are shown, in fact only one point out of every 4 % of total points are displayed. The species set as important are omitted as are the nitrogen sub-mechanism species and the ones that are absent at any of the selected points. Near the IDT, the number of species reaches its maximum and it may be observed that most hydrogen species remain at all points.

As could be seen in on Figure 17 (which presents normalized species molar fraction from Leplat's mechanism), hydrogen peroxide (H_2O_2) disappears after its molar fraction reaches a maximum and immediately before ignition. Species with more than 2 C atoms are not completely absent. Methanol is absent at almost all instants, appearing only at IDT. Aldehydes remain. Results at other conditions are similar.

4.5. Reduced Mechanism from Mittal's Base Mechanism

The DRG-sequential strategy did not perform well for Cancino's mechanism and therefore has not been used for Mittal's reduction. The methods employed for it were the DRG-parallel (named in this section only DRG) and the DRGEP. The final size of the reduced mechanism obtained from Mittal's detailed mechanisms can be observed on Table 11.

Table 11 - Total number of species and reactions for the Mittal reduced mechanisms

Mechanism	Number of Species	Numberof Reactions
Mittal (Base)	111	710
DRG	41 (37%)	240 (34%)
DRGEP	46 (41%)	303 (43%)

The DRG method achieved a greater reduction on the species number, when compared to the DRGEP method. This may be related with the difficult of the DRGEP method on handling kinetics mechanisms with several highly reactive intermediate species.

4.5.1. Reduction Targets Prediction

The main parameters used for comparison are the IDT for the conditions evaluated and the corresponding results can be observed in Figure 39, Figure 40 and Figure 41.

The reduced mechanisms predict the results of the detailed mechanism with excellent agreement. The difference between the mechanisms remains smaller than 5 %. Differently from the reduction of Cancino's mechanism, where the error was always smaller than 2 %, the reduction of Mittal´s mechanism stopped when the maximum difference reached the threshold allowed of 5% of IDT. This error on the ignition delay has some implications.

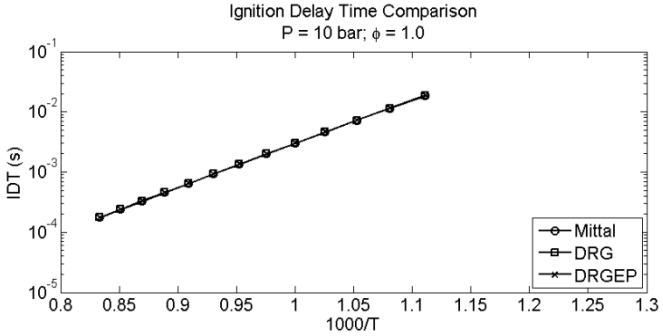

Figure 39 - IDT comparison of detailed kinetics mechanism of Mittal with the reduced mechanisms obtained via DRG and DRGEP. Pressure of 10 bar.

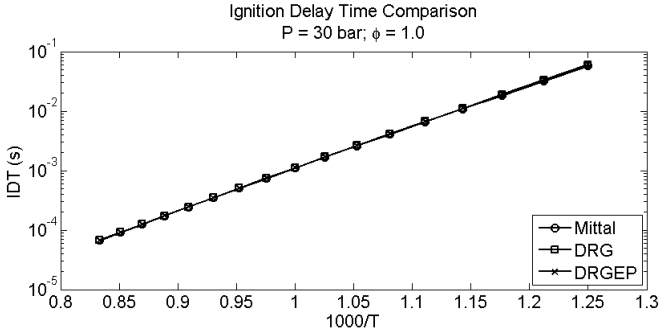

Figure 40 - IDT comparison of detailed kinetics mechanism of Mittal with the reduced mechanisms obtained via DRG and DRGEP. Pressure of 30 bar.

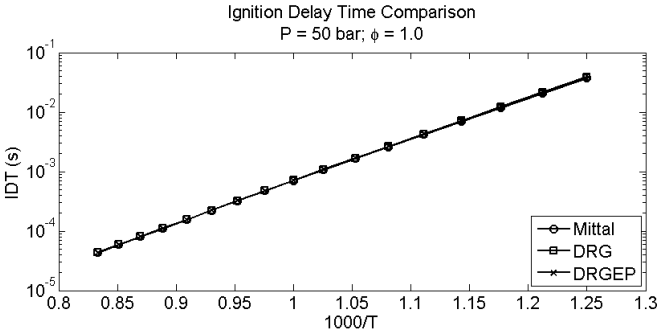

Figure 41 - IDT comparison of detailed kinetics mechanism of Mittal with the reduced mechanisms obtained via DRG and DRGEP. Pressure of 50 bar.

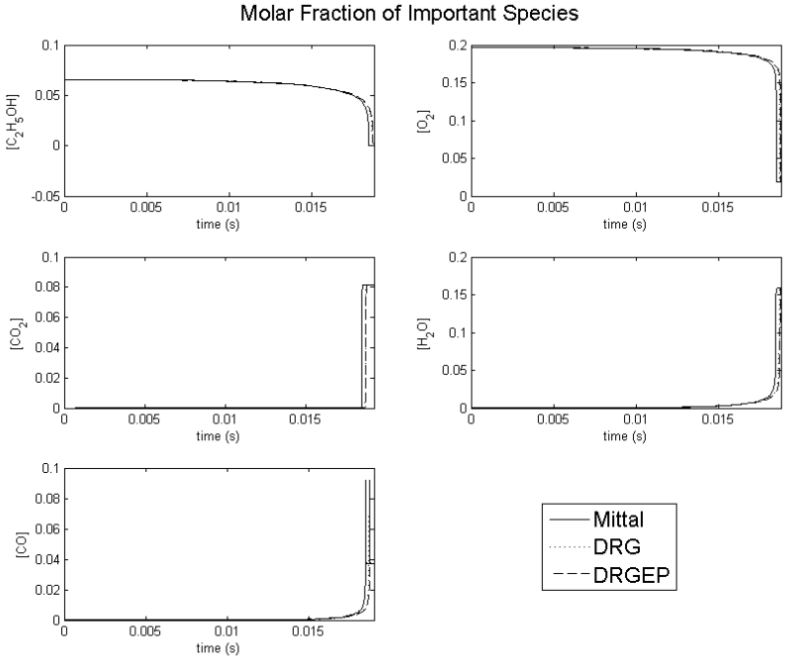

Figure 42 - Comparison of molar fraction of the important species for the IDT model at 10 bar and 900 K

Figure 42 presents the molar fraction of important species for the condition of 10 bar and 900 K. The DRG and DRGEP final reduced mechanisms are plotted against the results from the detailed mechanism. The IDT deviation near 5% results in a phasing of species concentration

profiles. Both reduced mechanisms present a higher IDT. The DRGEP method produced the mechanism with the larger deviation, which achieves almost 5 % when compared to the base solution while the DRG was kept under 3 %. This explains the small deviation of DRGEP concentration curves on Figure 42.

4.5.1. Rate of Reduction of the Different Reduction Methods

The reduction rates, presented on Table 12, illustrates the higher speed of the DRGEP method.

Table 12 - Reduction Speed Comparison (Mittal Reduced Mechanisms)

Method	**Iterations**	**Specie Removal Rate[1] (SRR)**	**Reaction Removal Rate[2] (RRR)**
DRG	19	3	24
DRGEP	9	7	45

[1] Number of total species removed divided by the iterations;
[2] Number of total reactions removed divided by the iterations.

Figure 43 presents the evolution of the reduction as the threshold increases. In the first step of 0.02, several species are flagged as unimportant for both methods. As expected, the slope of the reduction curve for the DRGEP is higher than that for DRG. Another aspect is that the reduction for DRG occurs by steps, not continually with the increase in threshold. This behavior creates a difficulty to automate the DRG method, since several tries must be performed with different thresholds to verify the continuation of the reduction process.

Using a one-step reduction with the DRG method and the final threshold of 0.16, the size of the reduced mechanism at each time step during the ignition may be observed in Figure 44. Contrary to Cancino, the size of this mechanism presents its maximum at the beginning of the ignition delay, decreasing the size as the thermochemical system evolves, and presenting another peak near ignition. This mechanism places more emphasis on early ignition phenomena than Cancino.

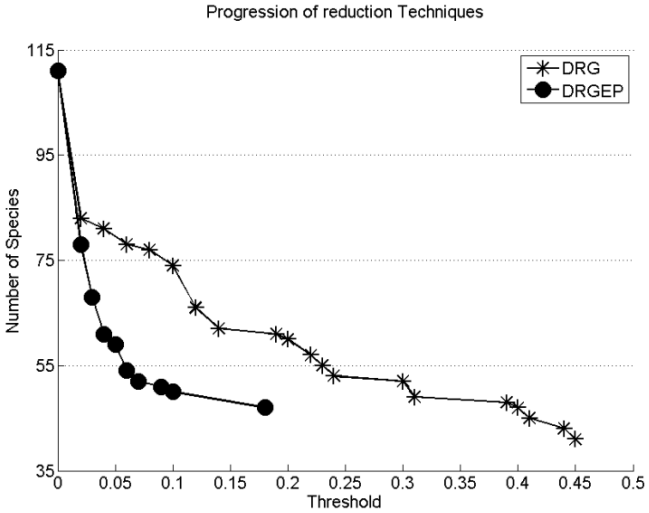

Figure 43 - Progression of different reduction techniques for the Mittal detailed Mechanism.

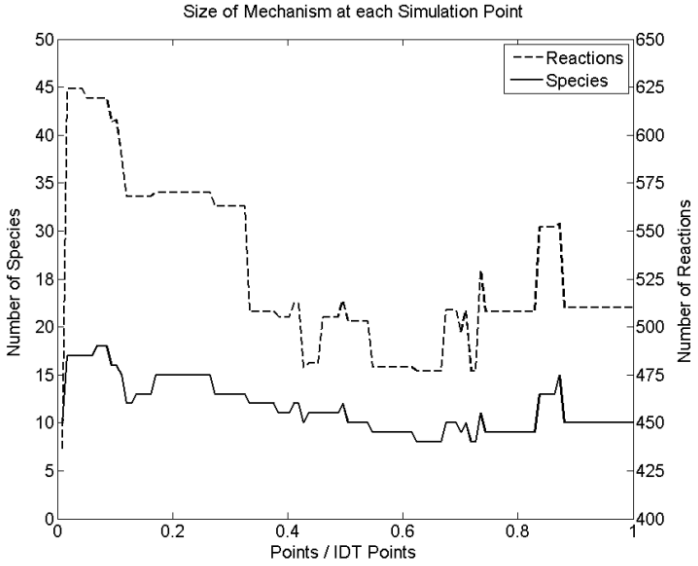

Figure 44 - Evolution of the Mechanism Size for a given condition and using an one-step DRG with a threshold of 0.16.

Point/IDT Points - From 0.01 to 1.00, steps of acc. 0.04

H	- x x x x x x x x x x x x x x x x x x x x
O	- - - - - - x x x x x x x x x x x x x x x
H2	- x x x x x x x x x x x x x x x x x x x x
HO2	x x x x x x x x x x x x x x x x x x x x x
H2O2	- - x x x x x x x - - - - - - - - - - - -
HCO	- x x x x x x x x x x x x x x x x x x x x
OCHO	- - - - - - - - - - - - - - - - - - x - -
OH*	- - - - - - - - - - - - - x - - - - x - -
C	- - - - - - - - - - - - - - - - - - x - -
CH2O	- x x x x x x x x x x x x x x x x x x x x
HOCH2O	- - - - - - - - - - - - - - - - - - - x x
HOCHO	- - - - x x x - - - - - - - - - - - - x x
CH3O	- - - x x x x x x - - - - - - - - - x - -
CH2OH	x x x x - - - - - - - x x x x - - x x x x
CH3OH	- - - - - - - - - - x - - - - - - - - -
CH3	x x x x x x x x x x x x x x x x x x x x x
CH4	- - x x x x x x x x x x x x x - - - - - -
HCOH	- x x - - - - - - - - - - - - - - - - - x x
CH2(S)	- x x - - - - - - - - x x x x x x - x x x x
CH	- - - - - - - - - - - - - - x x x - x - x x
C2H5	x x - - - - - x x x x - x x x x x x - - -
C2H6	- - - - - - - x x x x - x x x - - - - - - -
C2H4	x x x x x x x x x x x x x x x x x x x x x
C2H5O2	- - - - - - - - - - - - - - - - x - - - -
CH3CHO	- x x x x x x x x x x x x x x x x x x x -
C2H5O	- - - x x - - - - - - - - - - - - - - - -
C2H3O1-2	- - - - - - - - - - - x x x x x x x x x x
CH3CO	- - x x x x x x x x x x x x x x x x x x x
CH2CHO	- - - x x x x x x x x x x x x x x x x x x
CH2CO	- - - x x x x x x x x x x x x x x x - x x
HCCO	- - - x x x x x x x x x x x x x x x x x x
C2H3	- - - - - - - x x x x x x x x x x x x x x
C2H3OH	- x x x x - x x x x x x x x x x x x x x -
PC2H4OH	x x x x x x x x x x x x x x x - - - - - -
C2H2	- - - - - - - - x x x x x x x x x x x x x
C2H	- x
C3H3	- - - - - - - - - - - - - - - - x x x x x -
SC2H4OH	x x x x x x x x x x x x x x x x x x x x -
C2H5CHO	- - - - - - - - - - - - - - - - - x - - - -
CH3OCHO	- - - - - - - - - - - - - - - - - - - x - -
C3H4-P	- - - - - - - - - - - - - - - - - x x - - - -
C#CC*CCJ	- - - - - - - - - - - - - - - - - x x x x x -

Legend:
(x) is Present || (-) is Absent

Figure 45 - Presence of species on each simulation step till IDT for one condition using an one-step DRG for Mittal´s mechanism for 900 K and 10 bar.

Figure 45 presents the species that are removed in each time along ignition at 900 K and 10 bar. The threshold used was 0.16. The same rules used for the previous case (Figure 38, for the Cancino's species presence) are applied. The main differences are the number of points used until the IDT and the fact that there are no nitrogen species in the base mechanism. Also, the fact that the large number of species found on the initial steps presented on Figure 44 do not appear on Figure 45 is due to the fact that some of these species are needed only at a small number of points and could be omitted if these points were not selected as simulation points.

The hydrogen peroxide (H_2O_2) appears before IDT and after a small elapsed time it is removed from the mechanisms, as occurred with Cancino's mechanism. Several C and C2 species are needed in all the points. Some species, such as HO_2 and CH_2O, CH_3 and C_2H_4 are required during the entire oxidation process.

4.6. Sensitivity Analysis of the Reduced Mechanisms

The sensitivity analysis can be used as a mean to evaluate and find the reactions that must be studied and optimized to increase the accuracy of a given mechanism. During reduction, reactions are removed and this could affect the sensitivity of the remaining reactions.

The forthcoming sections present the comparison between the sensitivity coefficients for the original and reduced mechanisms.

4.6.1. Sensitivity Analysis for Leplat's Mechanisms

The final mechanism obtained via DRGEP was compared against the detailed mechanism. The flow rate sensitivity coefficients (laminar flame speed problem) for the 15th reactions with higher values (using the DRGEP as ranking parameter) can be observed on Figure 46.

In general, sensitivity coefficients are very similar for both cases, showing a significant correlation between the final reduced mechanism and the detailed one in respect to the most sensitivity reactions. However, several reactions change place on the sensitivity coefficients list.

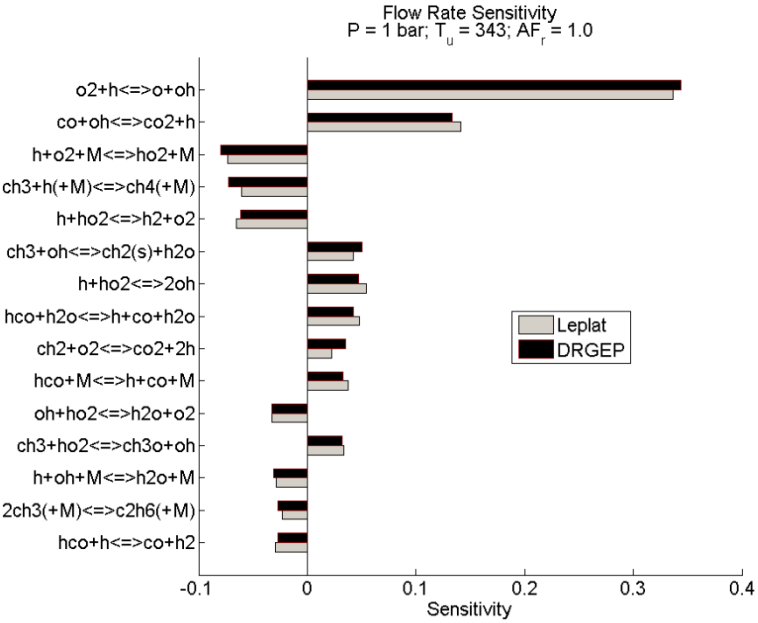

Figure 46 - Sensitivity for the Leplat and DRGEP mechanism for the 15th reactions with the higher sensitivity coefficients (ordered by the DRGEP mechanism) in respect to the flame speed.

4.6.2. Sensitivity for Cancino's Mechanism

For Cancino's Mechanism, the DRGEP reduced mechanism presented the greater reduction, while maintaining the same behavior presented by the detailed mechanism. The sensitivity of both mechanisms is presented on Figure 47 and Figure 48. Since the time step for the simulations is dynamically chosen by ChemKin, The comparison is done at a given elapsed time where both solutions are available.

The reactions with higher temperature sensitivity coefficients for the DRGEP mechanism are almost the same as those of the detailed one. The values of these coefficients are almost the same, showing that the core reactions for the temperature were kept in the final mechanism.

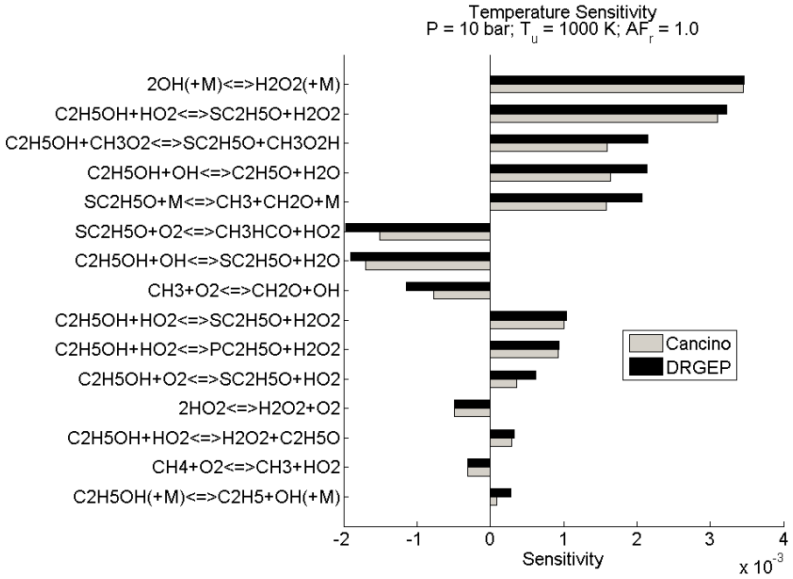

Figure 47 - Temperature sensitivity for 0.53 of IDT for Cancino mechanisms.

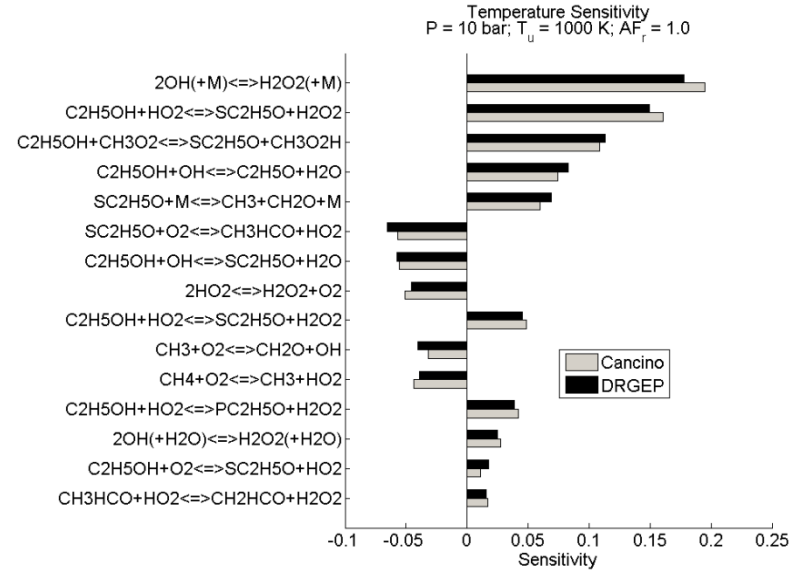

Figure 48 - Temperature sensitivity for 0.9 of IDT for Cancino mechanisms.

4.6.3. Sensitivity for the Mittal's Mechanism

The best reduced mechanism obtained from Mittal's detailed mechanism was generated by the DRG. The Temperature sensitivity coefficients for 10 bar of pressure and 1200 K (Ø = 1.0) and time of 0.56 and 0.91 of IDT is presented on Figure 49 and Figure 50.

The top reactions are almost the same for both DRG. The reactions used for optimization of the Mittal's mechanism are the same of those of the DRG reduced mechanism. The values of the sensitivities present small differences.

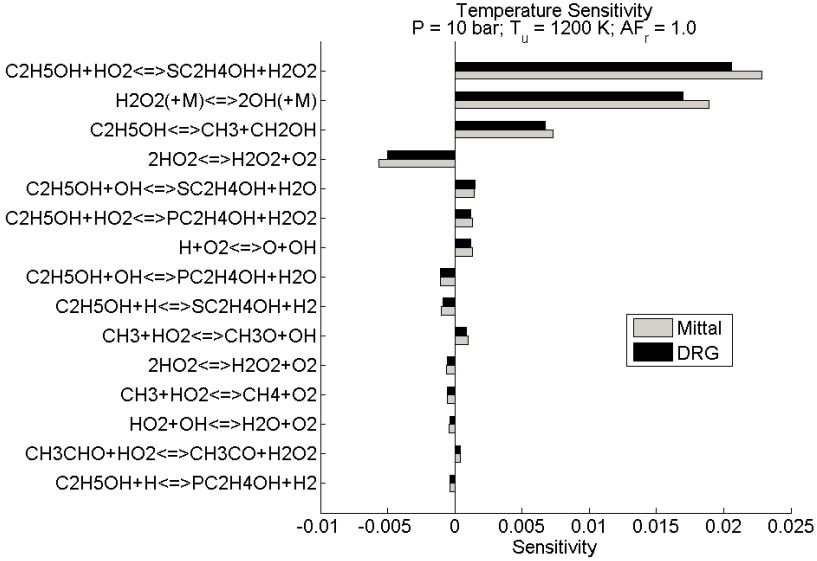

Figure 49 - Temperature sensitivity for 0.56 of IDT for Mittal mechanisms.

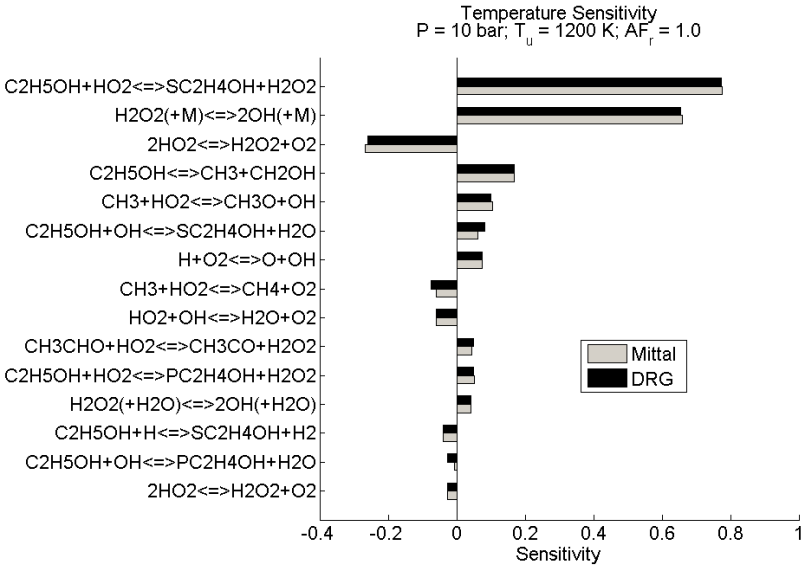

Figure 50 - Temperature sensitivity for 0.91 of IDT for Mittal mechanisms.

5. CONCLUSION

A reduced kinetics mechanism using DRGEP was obtained from the Leplat's detailed mechanism, presenting 32 species and 182 reactions, which represents a total of 84% of the species and 72% of the reactions of the original mechanism. The final mechanism reproduces flame speed results within deviations smaller than 5 %, for low pressure condition, and 25 % for the higher pressure condition. For IDT predictions, the deviation reached a maximum of 49 %.

Regarding Cancino's detailed mechanism, the DRGEP method lead to the smaller mechanism, with a total of 79 species and 821 reactions (including all the nitrogen oxidation mechanism), representing 58% and 61% of species and reactions respectively. The reduction was performed using IDT data with final deviations smaller than 2 %.

Concerning the Mittal's detailed mechanism, the final reduced mechanism was obtained via DRG, presenting 41 species and 240 reactions, corresponding to 37% and 34% of species and reactions respectively. The reduction was performed using IDT data, with final deviations smaller than 5 %.

When evaluating the performance of the reduced mechanisms obtained from Leplat's mechanism, the relevance of choosing the conditions and reactor models for the reduction is highlighted. Employing the reduced mechanism in different conditions from those used for obtaining it resulted in a solution with deviations above the limiting error (5 %) used for the reduction. This shows the great importance of choosing the adequate conditions for the reduction.

The reducing strategies that showed the best results, in terms of computational time (i.e. number of iterations) and efficiency (final size) were the species based methods, namely DRG and DRGEP. The DRGEP presented the best computational time of both and an overall greater efficiency, when compared to the DRG. The PFA however performed below the expectations for its nature.

The DSA method presents the largest reduction in respect to the number of reactions, although not in the species, and reproduced the detailed mechanism results with higher accuracy than the other methods. However, its application presents several complexities, and a large computational time is required. The ROP strategy performed poorly in comparison to all the other methods, achieving no species reduction.

Using the DRG as a tool to evaluate the mechanisms and a one-step reduction for both Cancino and Mittal mechanisms, the number of species necessary to describe the combustion process at each time step

was determined. One important difference is that, while Cancino's mechanism increases its size as the IDT approaches, Mittal's mechanism presents a larger mechanisms at the start of the process.

This difference on the behavior could be related to the different strategies used when assembling the mechanisms. Mittal's mechanism seems to have a larger complexity on the first steps of ethanol decomposition, whereas the Cancino's is more focused on the oxidation final steps.

One of the possible reasons that led the DRG to achieve a better result for the reduction of Mittal mechanism, when compared to the DRGEP, is the fact that the error propagation method find difficulty to handle a larger number of highly reactive species, condition found for Mittal's mechanism, but not observed in the same magnitude for Cancino and Leplat's mechanisms.

In respect to final mechanisms sensitivity, even achieving some high reduction rates, the reactions with larger sensitivities are the same in the reduced mechanisms with essentially the same coefficient value. This shows that the reduced mechanisms maintain the same core reactions, independently of the method employed.

For future works, some opportunities are pointed out:

1. To perform the reduction simultaneously using several different experiments as targets. This could increase the overall applicability of the reduced mechanism.
2. For the reduction of large kinetics mechanisms, e.g., mechanisms with thousands of species, the most suitable strategy is proven to be the DRGEP, since the number of iterations to achieve a large reduction is smaller than for the other methods. A hybrid strategy employing DRGEP, initially, and following with DSA could lead to even smaller mechanisms and still maintaining the relative error under a small limit.
3. To evaluate the use of on-the-fly reduction schemes as a way to reduce computational time for solving reactive flows in CFD while maintaining the accuracy of the chemical kinetics model.

6. REFERENCES

ALZUETA, M. U. and HERNÁNDEZ, J. M., Ethanol Oxidation and Its Interaction with Nitric Oxide. **Energy Fuels**, 2002, 16 (1), pp 166–171

BAHLOULI, K.; SARAY, R. K.; ATIKOL, U. Development of a Reduced Mechanism for n -Heptane Fuel in HCCI Combustion Engines by Applying Combined Reduction Methods. **Energy & Fuels,** [s.l.], v. 26, n. 6, p.3244-3256, 21 june 2012. American Chemical Society (ACS). DOI: 10.1021/ef300073n

BAHLOULI, K. et al. A reduced mechanism for predicting the ignition timing of a fuel blend of natural-gas and n-heptane in HCCI engine. **Energy Conversion and Management,** [s.l.], v. 79, p.85-96, mar. 2014. Elsevier BV. DOI: 10.1016/j.enconman.2013.12.005.

BORISOV, A. A., ZAMANSKII, V. M., KONNOV, A. A., LISYANKII, V. V., RUSAKOV, S. A. and SKACHKOV, G. I., High-temperature pyrolysis of ethanol. **Soviet Journal of Chemical Physics**, 8, 1991, pp. 121-141.

BP. BP Statistical Review of World Energy 2015. **British Petroleum**. Ed 64. 2015. Available at http://www.bp.com/content/dam/bp /pdf/energy-economics/statistical-review-2015/

CANCINO, L. R. **Desenvolvimento e Aplicação de Modelos Cinéticos Detalhados para Etanol e Combustíveis Hidrocarbonetos Contendo Etanol.** 2009. 130 f. Tesis (Doctor Degree) - Curso de Engenharia Mecânica, Programa de Pós-graduação em Engenharia Mecânica, Universidade Federal de Santa Catarina, Florianópolis, 2009.

CANCINO, L. R. et al. Measurement and Chemical Kinetics Modeling of Shock-Induced Ignition of Ethanol−Air Mixtures. **Energy & Fuels,** [s.l.], v. 24, n. 5, p.2830-2840, 20 may 2010. American Chemical Society (ACS). DOI: 10.1021/ef100076w.

CHEMKIN-PRO 15083, Reaction Design: San Diego, 2009.

CURRAN, H. J., DUNPHY, M. P., SIMMIE, J. M., WESTBROOK, C.K. and PITZ, W.J., Shock tube ignition of ethanol, isobutene and

MTBE: Experiments and modeling, **Proceedings of the Combustion Institute**, 24, 1992, pp. 833-841.

DAGAUT, P., BOETTNER, J.C. and CATHONNET, M., Kinetic modeling of ethanol pyrolysis and combustion, **Journal de Chimie Physique**, 89, 1992, pp. 867-884.

DAGAUT, P.; TOGBÉ, C. Experimental and Modeling Study of the Kinetics of Oxidation of Ethanol−Gasoline Surrogate Mixtures (E85 Surrogate) in a Jet-Stirred Reactor. **Energy & Fuels,** [s.l.], v. 22, n. 5, p.3499-3505, 17 sept. 2008. American Chemical Society (ACS). DOI: 10.1021/ef800214a.

DEMÉTRIO, M. J. E. **Análise de Mecanismos Cinéticos para a Combustão de Etanol.** 2013. 182 f. Dissertação (Mestrado) - Curso de Engenharia Mecânica, Programa de Pós-graduação em Engenharia Mecânica, Universidade Federal de Santa Catarina, Florianópolis, 2013.

DUNPHY, M. P.; SIMMIE, J. M.. High-temperature oxidation of ethanol. Part 1.Ignition delays in shock waves. **Faraday Trans.,** [s.l.], v. 87, n. 11, p.1691-1696, 1991. Royal Society of Chemistry (RSC).

DUNPHY, M. P.; PATTERSON, P. M.; SIMMIE, J. M.. High-temperature oxidation of ethanol. Part 2.Kinetic modelling. **Faraday Trans.,** [s.l.], v. 87, n. 16, p.2549-2559, 1991. Royal Society of Chemistry (RSC).

EGOLFOPOULOS, F.N., D.X. DU, C.K. LAW, A study on ethanol oxidation kinetics in laminar premixed flames, flow reactors, and shock tubes, **Symposium (International) on Combustion**, Volume 24, Issue 1, 1992, Pages 833-841

EGOLFOPOULOS, F.N., HANSEN N., JU Y., KOHSE-HÖINGHAUS K., LAW C.K., QI F., Advances and challenges in laminar flame experiments and implications for combustion chemistry, **Progress in Energy and Combustion Science**, Volume 43, August 2014, Pages 36-67

EIA. Annual Energy Outlook 2014, with projections to 2040. **U.S. Energy Information Administration**. DOE/EIA – 0383, 2014. Available at http://www.eia.gov/forecasts/aeo/

EIA. Liquid Fuels and Natural Gas in the Americas**. U.S. Energy Information Administration.** 2014. Available at http://www.eia.gov/countries/americas/

EPE (Brazil). Balanço Energético Nacional 2013: Ano base 2012. **Empresa de Pesquisa Energética**. Rio de Janeiro: EPE, 2013.

MAAS, U. and POPE, S. B.. Simplifying chemical kinetics: intrinsic low-dimensional manifolds in composition space. **Combustion and Flame**, v. 88, n. 3-4, p 239-264, mar 1992.

GLARBORG, P.; MILLER, J. A.; KEE, R. J.. Kinetic modeling and sensitivity analysis of nitrogen oxide formation in well-stirred reactors. **Combustion and Flame,** [s.l.], v. 65, n. 2, p.177-202, aug. 1986. Elsevier BV. DOI: 10.1016/0010-2180(86)90018-0.

GOU, X. et al. A dynamic adaptive chemistry scheme with error control for combustion modeling with a large detailed mechanism. **Combustion And Flame,** [s.l.], v. 160, n. 2, p.225-231, feb. 2013. Elsevier BV. DOI: 10.1016/j.combustflame.2012.10.015.

GULDER, O.L., Laminar burning velocities of methanol, ethanol, and isooctane -air mixtures, **Proceedings Commbustion Institute**, 19, 1982, pp. 275-281.

HERNÁNDEZ, J. J.; BALLESTEROS, R.; SANZ-ARGENT, J.. Reduction of kinetic mechanisms for fuel oxidation through genetic algorithms. **Mathematical and Computer Modelling,** [s.l.], v. 52, n. 7-8, p.1185-1193, oct. 2010. Elsevier BV. DOI: 10.1016/j.mcm.2010.02.035

HERRMANN, F., JOCHIM, B., OSSWALD, P., CAI, L., PITSCH, H., KOHSE-HOINGHAUS, K., Experimental and numerical low-temperature oxidation study of ethanol and dimethyl ether, **Combustion and Flame**, 161 (2014) 384-397.

JEULAND, N., MONTAGNE, X.; GAUTROT, X. Potentiality of Ethanol as a Fuel for Dedicated Engine. **Oil & Gas Science and Technology** – Rev. IFP, v. 59, pp 559-570. 2004.

KALGHATGI, G. T. The Outlook for fuels for internal combustion engines. **International Journal of Engine Research**. v. 15, pp 383-398, 2014.

KARADENIZ, H.; SOYHAN, H. S.; SORUSBAY, C.. Reduction of large kinetic mechanisms with a new approach to the necessity analysis method. **Combustion and Flame,** [s.l.], v. 159, n. 4, p.1467-1480, apr. 2012. Elsevier BV. DOI: 10.1016/j.combustflame.2011.11.011

KOKJOHN, S. L., HANSON, R. M., SPLITTER, D. A., REITZ, R. D. Fuel reactivity controlled compression ignition (RCCI): a pathway to controlled high-efficiency clean combustion. **International Journal of Engine Research,** v. 12, pp. 209-226, 2011.

KONNOV, A. A.; MEUWISSEN, R. J.; GOEY, L. P. H. The temperature dependence of laminar burning velocity of ethanol flames. **Proceedings of the Combustion Institute**, v. 33, pp. 1011-1019, 2011.

LAM, S. H..; GOUSSIS, D. A... Understanding complex chemical kinetics with computational singular perturbation. **Symposium (international) on Combustion,** [s.l.], v. 22, n. 1, p.931-941, jan. 1989. Elsevier BV. http://dx.doi.org/10.1016/s0082-0784(89)80102-x.

LEBEDEV, A. V. et al. Systematic procedure for reduction of kinetic mechanisms of complex chemical processes and its software implementation. **Journal of Mathematical Chemistry,** [s.l.], v. 51, n. 1, p.73-107, 11 aug. 2012. Springer Science + Business Media. DOI: 10.1007/s10910-012-0065-z.

LEPLAT, N. et al. Numerical and experimental study of ethanol combustion and oxidation in laminar premixed flames and in jet-stirred reactor. **Combustion and Flame,** [s.l.], v. 158, n. 4, p.705-725, apr. 2011. Elsevier BV. DOI: 10.1016/j.combustflame.2010.12.008.

LI, J. Experimental and numerical studies of ethanol chemical kinetics, Ph.D. Thesis, Princeton University, 2004.

LI J., KAZAKOV A., CHAOS M., DRYER F. L., Chemical kinetics of ethanol oxidation, **Proceedings of the 5th US Combustion Meeting**, 2007, pp. 1-16.

LI, S.; JIANG, Y.; QIU, R.. The Generation of a Reduced Mechanism for Flame Inhibition by Phosphorus Containing Compounds Based on Path Flux Analysis Method. **Chinese Journal of Chemical Engineering,** [s.l.], v. 21, n. 4, p.357-365, apr. 2013. Elsevier BV. DOI: 10.1016/s1004-9541(13)60480-2.

LIU, A. et al. Flux Projection Tree Method for Mechanism Reduction. **Energy & Fuels,** [s.l.], v. 28, n. 8, p.5426-5433, 21 aug. 2014. American Chemical Society (ACS). DOI: 10.1021/ef5002502.

LU, T.; LAW, C. K.. A directed relation graph method for mechanism reduction. **Proceedings of the Combustion Institute,** [s.l.], v. 30, n. 1, p.1333-1341, jan. 2005. Elsevier BV. DOI: 10.1016/j.proci.2004.08.145.

LU, T.; LAW, C. K.. Linear time reduction of large kinetic mechanisms with directed relation graph: n-Heptane and iso-octane. **Combustion and Flame,** [s.l.], v. 144, n. 1-2, p.24-36, jan. 2006a. Elsevier BV. DOI: 10.1016/j.combustflame.2005.02.015.

LU, T.; LAW, C. K.. On the applicability of directed relation graphs to the reduction of reaction mechanisms. **Combustion and Flame,** [s.l.], v. 146, n. 3, p.472-483, aug. 2006b. Elsevier BV. DOI: 10.1016/j.combustflame.2006.04.017.

LUO, Zhaoyu et al. A Reduced Mechanism for High-Temperature Oxidation of Biodiesel Surrogates. **Energy & Fuels,** [s.l.], v. 24, n. 12, p.6283-6293, 16 dez. 2010. American Chemical Society (ACS).

MARINOV N.M. (1999) : A detailed chemical kinetic model for high temperature ethanol oxidation, **International Journal of Chemical Kinetics**, vol. 31, pp. 183-220.

MATLAB Release 2012a, The MathWorks, Inc., Natick, Massachusetts, United States.

MITTAL, G. et al. Autoignition of ethanol in a rapid compression machine. **Combustion and Flame,** [s.l.], v. 161, n. 5, p.1164-1171, may 2014. Elsevier BV. DOI: 10.1016/j.combustflame.2013.11.005.

NATARAJAN K., BHASKARAM K.A. "An experimental and analytical investigation of high temperature ignition of ethanol." **Proc 13th Int. Shock Tube Symp.**, Niagara Falls, pp. 834. (1981).

NIEMEYER, K. E.; SUNG, C.; RAJU, M. P.. Skeletal mechanism generation for surrogate fuels using directed relation graph with error propagation and sensitivity analysis. **Combustion and Flame,** [s.l.], v. 157, n. 9, p.1760-1770, sept. 2010. Elsevier BV. DOI: 10.1016/j.combustflame.2009.12.022.

NORTON, T.S. and DRYER, F.L., An experimental and modeling study of ethanol oxidation, **International Journal of Chemical Kinetics**, 31, 1999, pp.183-220.

OKUYAMA, M. et al. Development of an Ethanol Reduced Kinetic Mechanism Based on the Quasi-Steady State Assumption and Feasibility Evaluation for Multi-Dimensional Flame Analysis. **Journal of Thermal Science and Technology,** [s.l.], v. 5, n. 2, p.189-199, 2010. Japan Society of Mechanical Engineers. DOI: 10.1299/jtst.5.189

ORBEGOSO, E. M. M., FIGUEIRA DA SILVA, L .F. and NOVGORODCEV ,Jr., A. R., **On The Predictability of Chemical Kinetics for the Description of the Combustion of Simple Fuels**, J. of the Braz. Soc. of Mech. Sci. & Eng., October-December 2011, Vol. XXXIII, No. 4, pp. 492-505.

PARK, J.; ZHU, R. S.; LIN, M. C.. Thermal decomposition of ethanol. I. Ab Initio molecular orbital/Rice–Ramsperger–Kassel–Marcus prediction of rate constant and product branching ratios. **The Journal of Chemical Physics,**[s.l.], v. 117, n. 7, p.3224-3231, 2002. AIP Publishing.

PARK, J.; XU, Z. F.; LIN, M. C.. Thermal decomposition of ethanol. II. A computational study of the kinetics and mechanism for the H+C2H5OH reaction. **The Journal of Chemical Physics,** [s.l.], v. 118, n. 22, p.9990-9996, 2003. AIP Publishing.

PEPIOTDESJARDINS, P; PITSCH, H. An efficient error-propagation-based reduction method for large chemical kinetic mechanisms. **Combustion and Flame,** [s.l.], v. 154, n. 1-2, p.67-81, july. 2008. Elsevier BV. DOI: 10.1016/j.combustflame.2007.10.020.

QIN, Z. et al. Combustion chemistry of propane: A case study of detailed reaction mechanism optimization. **Proceedings of The Combustion Institute,** [s.l.], v. 28, n. 2, p.1663-1669, jan. 2000. Elsevier BV.

REITZ, R. D., Combustion and ignition chemistry in internal combustion engines. **International Journal of Engine Research**. v.14, pp. 411-415, 2013.

ROHL, O. and PETERS, N., 2007, A Reduced Mechanism for Ethanol Oxidation, **Proceedings of the European Combustion Meeting**, pp. 1-5.

SARATHY S. M., OßWALD P., HANSEN N., KOHSE-HÖINGHAUS K., Alcohol combustion chemistry, **Progress in Energy and Combustion Science**, Volume 44, October 2014, Pages 40-102

SAXENA P., WILLIAMS F.A. (2007) : Numerical and experimental studies of ethanol flames, **Proceedings of the Combustion Institute**, vol. 31, pp. 1149-1156.

SHI, Y. et al. Automatic Chemistry Mechanism Reduction of Hydrocarbon Fuels for HCCI Engines Based on DRGEP and PCA Methods with Error Control. **Energy & Fuels,** [s.l.], v. 24, n. 3, p.1646-1654, 18 mar. 2010. American Chemical Society (ACS). DOI: 10.1021/ef901469p.

SUN, W. et al. A path flux analysis method for the reduction of detailed chemical kinetic mechanisms. **Combustion and Flame,** [s.l.], v. 157, n. 7, p.1298-1307, july. 2010. Elsevier BV. DOI: 10.1016/j.combustflame.2010.03.006.

SUNG C., CURRAN H. J., Using rapid compression machines for chemical kinetics studies, **Progress in Energy and Combustion Science**, Volume 44, October 2014, Pages 1-18

TOSATTO, L.; BENNETT, B. A. V.; SMOOKE, M. D. A transport-flux-based directed relation graph method for the spatially inhomogeneous instantaneous reduction of chemical kinetic mechanisms. **Combustion and Flame,** [s.l.], v. 158, n. 5, p.820-835, may 2011. Elsevier BV. DOI: 10.1016/j.combustflame.2011.01.018.

TOSATTO, L.; BENNETT, B. A. V..; SMOOKE, M. D...Comparison of different DRG-based methods for the skeletal reduction of JP-8 surrogate mechanisms. **Combustion and Flame,** [s.l.], v. 160, n. 9, p.1572-1582, sept. 2013. Elsevier BV. DOI: 10.1016/j.combustflame.2013.03.024.

TRAN, L. et al. Experimental and Modeling Study of Premixed Laminar Flames of Ethanol and Methane.**Energy & Fuels,** [s.l.], v. 27, n. 4, p.2226-2245, 18 apr. 2013. American Chemical Society (ACS). DOI: 10.1021/ef301628x.

TURNS, S. R. . **Introdução à Combustão:** conceitos e aplicações. 3. ed. Porto Alegre: AMGH, 2013. 404 p. Translation: Amir Antônio Martins de Oliveira Júnior.

XU, Z. F.; PARK, J.; LIN, M. C.. Thermal decomposition of ethanol. III. A computational study of the kinetics and mechanism for the CH3+C2H5OH reaction. **The Journal of Chemical Physics,** [s.l.], v. 120, n. 14, p.6593-6599, 2004. AIP Publishing

WARNATZ, J.; MAAS, U.; DIBBLE, R. W. .**Combustion: Physical and Chemical Fundamentals, Modeling and Simulation, Experiments, Pollutant Formation**. 4. ed. Berlin: Springer, 2006. 377 p.

ZHANG, S.; ANDROULAKIS, I. P.; IERAPETRITOU, M. G.. A hybrid kinetic mechanism reduction scheme based on the on-the-fly reduction and quasi-steady-state approximation. **Chemical Engineering Science,**[s.l.], v. 93, p.150-162, apr. 2013. Elsevier BV. DOI: 10.1016/j.ces.2013.01.066.

ZHAO Z., CHAOS M., KAZAKOV A. and DRYER F. L., Thermal decomposition reaction and a comprehensive kinetic model of dimethyl ether, **International Journal of Chemical Kinetics**, Vol 40, 2008, pp 1–18.